A THESIS SUBMITTED TO
THE GRADUATE SCHOOL OF NATURAL AND APPLIED SCIENCES
OF ÇANKIRI KARATEKİN UNIVERSITY

INVESTIGATION OF SPECTROSCOPIC AND NONLINEAR OPTICAL (NLO) PROPERTIES OF N^2 ,N^6 -BIS-[4-(AMINOSULFONYL) PHENYL]-PYRIDINE-2,6-DICARBOXAMIDE BY DFT METHOD

IN PARTIAL FULFILLMENT OF THE REQUIREMENTS
FOR
THE DEGREE OF MASTER OF SCIENCE
IN
PHYSICS

BY

HASANAIN ABDULKAREEM ABBAS AL-HADMAWI

ÇANKIRI

2022

INVESTIGATION OF SPECTROSCOPIC AND NONLINEAR OPTICAL (NLO) PROPERTIES OF N^2 ,N^6 -BIS-[4-(AMINOSULFONYL) PHENYL]-PYRIDINE-2,6-DICARBOXAMIDE BY DFT METHOD

By Hasanain Abdulkareem Abbas AL-HADMAWI

October 2022

We certify that we have read this thesis and that in our opinion it is fully adequate, in scope and in quality, as a thesis for the degree of Master of Science

Advisor : Prof. Dr. Hamit ALYAR

Examining Committee Members:

Chairman : Prof. Dr. Mustafa Kemal ÖZTÜRK
Physics
Gazi University

Member : Prof. Dr. Hamit ALYAR
Physics
Çankırı Karatekin University

Member : Assoc. Prof. Dr. İlyas İNCİ
Physics
Çankırı Karatekin University

Approved for the Graduate School of Natural and Applied Sciences

Prof. Dr. İbrahim ÇİFTÇİ
Director of Graduate School

I hereby declare that all information in this document has been obtained and presented in accordance with academic rules and ethical conduct. I also declare that, as required by these rules and conduct, I have fully cited and referenced all material and results that are not original to this work.

Hasanain Abdulkareem Abbas AL-HADMAWI

ABSTRACT

INVESTIGATION OF SPECTROSCOPIC AND NONLINEAR OPTICAL (NLO) PROPERTIES OF N^2 ,N^6 -BIS-[4-(AMINOSULFONYL) PHENYL]-PYRIDINE-2,6-DICARBOXAMIDE BY DFT METHOD

Hasanain Abdulkareem Abbas AL-HADMAWI

Master of Science in Physics

Advisor: Prof. Dr. Hamit ALYAR

October 2022

Sulfonamides are organic sulfur compounds containing -SO_2NH_2 group, and they are compounds with antimicrobial activity and antibacterial activity that prevent the growth of bacteria. The discovery of sulfonamides is an important milestone in human chemotherapeutic history. In 1935, it was found that the dye prontosil was metabolized in vivo to an active compound, sulfanilamide, and this active compound prevented streptococcal infections in mice. In this thesis, the stable structure of N^2,N^6-bis-[4-(aminosulfonyl)phenyl]-pyridine-2,6-dicarboxamide compound synthesized by Adem Rıza BAYKAN was obtained by DFT method by performing geometry optimization calculation at B3LYP/6-311++G(d,p) level. Since the molecule studied in the literature has no experimental structural parameters, the theoretically calculated bond lengths and bond angles of the compound were compared with the experimental values of similar molecules in the literature. Especially S-O, S-N and N-C bond lengths were calculated as 1.461, 1.695 and 1.382 Å, and it was seen that the calculated results were compatible with the experimental values in the literature. In addition, the spectroscopic properties of the molecule such as FT-IR, ^{1}H-NMR and ^{13}C-NMR were calculated with the same method and basis set. In the obtained FT-IR analysis results, it is seen that the values of 1263 and 1261 cm-1 calculated for the C-N stretching vibration coincide with the values of similar molecular groups in the literature. Finally, the HOMO and LUMO energies of the molecule at the B3LYP/6-311++G(d,p) level were calculated by the DFT method. The obtained HOMO and LUMO energy difference was found to be 4.685 eV. The nonlinear optical properties and molecular potential energy surface map of the studied

compound were calculated using the same method and basis set. As a result of calculation, the compound was found to have a hyperpolarizability of 2665.2×10^{-33} esu. This value indicates that the hyperpolarizability of the compound is approximately 7.15 times greater than that of urea. In this thesis study, all calculations were performed with Gaussian 09 (Linux) and Gauss View 5.0 package programs.

2022, 71 pages

Keywords: FT-IR, NMR, NLO, DFT, HOMO, LUMO

ÖZET

N^2 ,N^6 -BİS-[4-(AMİNOSÜLFONİL)FENİL]-PİRİDİN-2,6-DİKARBOKSAMİT BİLEŞİĞİNİN SPEKTROSKOPİK VE DOĞRUSAL OLMAYAN OPTİK (NLO) ÖZELLİKLERİNİN DFT METODUYLA İNCELENMESİ

Hasanain Abdulkareem Abbas AL-HADMAWI

Fizik, Yüksek Lisans

Tez Danışmanı: Prof. Dr. Hamit ALYAR

Ekim 2022

Sülfonamitler, $-SO_2NH_2$ grubu içeren organik sülfür bileşikler olup, bakterilerin büyümesini önleyen antibakterial aktiviteye sahip, antimikrobiyal özellik gösteren bileşiklerdir. Sülfonamidlerin keşfi insan kemoterapatik tarihinin önemli bir dönüm noktasıdır. 1935 yılında prontosil adlı boyanın in vivo olarak aktif bir bileşik olan süfanilamid'e metabolize olduğu ve bu aktif bileşiğin farelerdeki streptokok enfeksiyonlarını önlediği bulunmuştur. Bu tez çalışmasında Adem Rıza BAYKAN tarafından sentezlenenN^2,N^6-bis-[4-(aminosulfonyl)phenyl]-pyridine-2,6-dicarboxamide bileşiğinin kararlı yapısı DFT metodu ile B3LYP/6-311++G(d,p) seviyesinde geometri optimizasyon hesabı yapılarak elde edildi. Literatürde çalışılan molekülün deneysel yapısal parametreleri olmadığı için bileşiğin teorik olarak hesaplanan bağ uzunlukları ve bağ açıları literatürdeki benzer moleküllerin deneysel değerleriyle karşılaştırıldı. Özellikle S-O, S-N ve N-C bağ uzunlukları 1.461, 1.695 and 1.382 Å olarak hesaplandı ve hesaplanan sonuçların literatürdeki deneysel değerler ile uyumlu olduğu görüldü. Ayrca molekülün FT-IR, ^{1}H-NMR ve ^{13}C-NMR gibi spektroskopik özellikleri yine aynı metot ve temel set ile hesaplandı. Elde edilen FT-IR analizi sonuçlarında C-N gerilme titreşimi için hesaplanan 1263 ve 1261 cm^{-1} değerlerinin literatürdeki benzer molekül gruplarına ait değerlerle örtüştüğü görülmektedir. Son olarak molekülünün DFT metodu ile B3LYP/6-311++G(d,p) seviyesinde HOMO ve LUMO enerjileri hesaplandı. Elde edilen HOMO ve LUMO enerji farkı 4.685 eV olarak bulundu. Yine aynı metot ve temel set kullanılarak çalışılan bileşiğin çizgisel omayan optiksel özelliği ve moleküler potansiyel enerji yüzey haritası hesaplandı. Hesaplama sonucunda bileşiğin 2665.2 x10^-

^{33} esu değerinde bir hiperpolarizebiliteye sahip olduğu bulundu. Bu değer bileşiğin hiperpolarizebilitesinin üreden yaklaşık olarak 7.15 kat daha büyük olduğunu göstermektedir. Bu tez çalışmasında hesaplamaların tamamı Gaussian 09(Linux) ve Gauss View 5.0 pakaet programlarıyla gerçekleştirildi.

2022, 71 sayfa

Anahtar Kelimeler: FT-IR, NMR, NLO, DFT, HOMO, LUMO

PREFACE AND ACKNOWLEDGEMENTS

I would like to thank Prof. Dr. Hamit ALYAR, who is my thesis advisor, for his understanding, patience, and mentoring. He taught me a lot of things. I ask Allah to keep him safe. I do not forget my father who supported me with prayers and my brothers and my friends ,all my loved ones and those who helped me. I do not forget my beloved deceased mother, who is lying under the dirt. And I know she prays for me in heaven.

Hasanain Abdulkareem Abbas AL-HADMAWI

Çankırı-2022

CONTENTS

LIST OF SYMBOLS

ε_r	Dielectric constant
μ_o	The permeability of free space or vacuum
C	Speed of light
$\hat{H}$	Hamiltonian processor
h	Planck constant
K	Wavenumber
t	Twisting
α_{ave}	Polarizability
β	In-plane angle bending
β_{tot}	Hyperpolarizability
δs	Scissoring
E	Energy eigen value
ε_0	The permittivity of free space or vacuum
λ	Wavelengith
ν_{as}	Asymmetric stretching
ν_s	Symmetric stretching
P	Total electron density
σi	Spin coordinate
Ψ	Wave function
ω	Wagging vibration
γ	Out of plane bending
δ	Bending vibrations (deformations)
ν	Stretching vibrations
ρ	Rocking vibration
τ	Torsion vibration

LIST OF ABBREVIATIONS

AAS	Atomic absorption spectroscopy
DFT	Density Functional Theory
DHPS	Deoxyhypusine synthase
EMR	Electromagnetic-radiation
EPR	Electron paramagnetic resonance
ESR	Electron spin resonance
HF	Hartree Fock
HF	High frequency
HIV	Human immunodeficiency virus
LIGO	Laser Interferometric Gravitational Wave Observatory
NLO	Nonlinear optical
NMR	Nuclear magnetic resonance
PES	Potential energy surface
RF	Radio frequency
SCF	Self consistent field

LIST OF FIGURES

LIST OF TABLES

1. INTRODUCTION

Sulfa medicines were the first chemically manufactured antimicrobials, and they're still used to treat a variety of bacterial, protozoal, and fungal illnesses (Wolff 1996, Scozzafava *et al.* 2000). With The popularity of penicillin and other antibiotics The amount of sulfonamides in the body has been reduced. They are, nevertheless, still used as sulfa medicines. in some cases, include sulfamerazine, sulfadiazine, and sulfathiazole. In therapeutic domains, particularly in ocular infections, they are also used to treat urinary tract and gastrointestinal infections (singh *et al.* 1994).

Chemically, compounds containing the SO_2NH_2 functional group are called sulfonamides. The general formula of sulfonamides is RSO_2NH_2 (Lavanya 2017). The chemical structure of the sulfonamide is shown in (Figure 1.1).

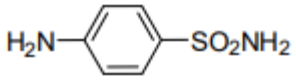

Figure 1.1 The general formula of sulfonamide is RSO_2NH_2 (Lavanya 2017)

In the structure of the sulfonamides , the amino group and sulfonyl groups on the benzene ring are in paraposition relative to each other. The nitrogen atom's associated groups in the sulfonamide functional group change the potency of the compound. If other rings are used instead of the benzene ring, changes will occur in the substitution and activity properties of the molecule. The lipophilicity of the sulfonamide group has a very important role in binding the molecule to protein. The best results can be obtained by replacing a hydrogen of the 1. $-NH_2$ group in the first position with heterocyclic rings. However, in order to be effective on bacteria, the para amino group must be free in the molecule. In sulfonamides, the $–NH_2$ group in the para position can be replaced by $–NO_2$, –NHOH, and –N=N groups (Kolaczek *et al.* 2014).

The nitrogen atom in the sulfonamide structure is classified as primary, secondary, and tertiary according to the number of groups that are associated with it. The classification of sulfonamides is shown in (Figure 1.2) Primary (sulfonamides) contain 2 H atoms on the nitrogen atom attached to the sulfony l group; secondary sulfonamides contain 1H atom; and tertiary sulfonamides do not contain H atoms. Primary and secondary sulfonamides show acidic properties because they contain H atoms, while tertiary sulfonamides do not show acidic properties because they do not contain H atoms (Moeker *et al.* 2014).

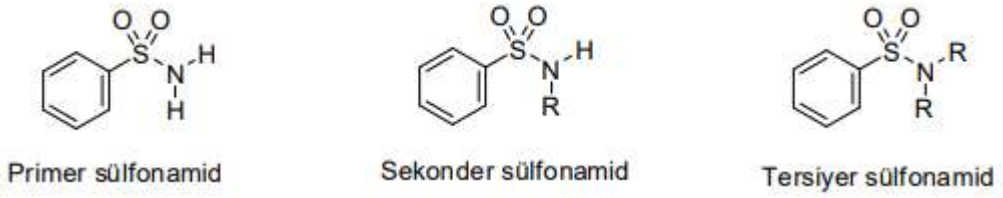

Figure 1.2 General structure of primary, secondary and tertiary sulfonamides (Moeker *et al.* 2014)

Gram (-) bacteria are more resistant to aliphatic sulfonamides than Gram (+) bacteria, and the antibacterial efficacy declines with increasing carbon chain length. In addition, it is known that macrocyclic bis-sulfonamides show antimicrobial activities (Kolaczek *et al.* 2014).

Classical sulfonamides, which are DHPS (dihydropteroate synthase) enzyme inhibitors, are broad-spectrum antibiotics and have been used in the treatment of many infections for many years due to their low cost and low toxicity (Aslan 2017). Due to the resistance of bacteria, it is mostly used in urinary tract infections, toxoplasmosis, and nocardiosis infections in the form of mixtures combined with dihydrofolate reductase inhibitors such as trimethoprim, tetroxoprim, or diaminopyrimidine. The new generation sulfonamides obtained by attaching different groups and substituents to the $-SO_2NH_2$ functional group have different enzyme inhibitory properties. they show. For example, Sildenafil Citrate (Viagra®) (Brock 2000). which is a PDE5 (phosphodiesterase type 5) inhibitor, Amprenavir (Agenerase®) which is an HIV-I aspartyl protease inhibitor and used in the treatment of AIDS (Adkins and Faulds 1998,

Meyers *et al.* 1972), Celecoxib (Celebrex®) (Penning *et al.* 1997) can be given in the treatment of osteoarthritis and rheumatoid arthritis, which is a COX-2 inhibitor (Figure 1.3).

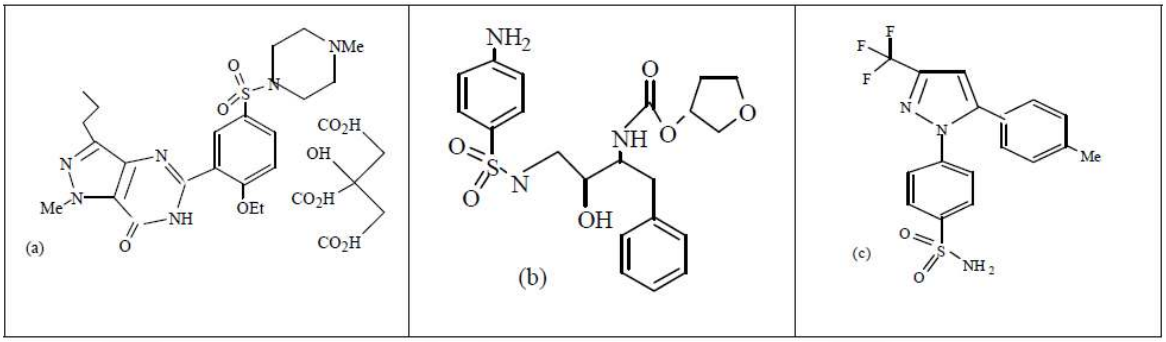

Figure 1.3 Some new generation Sulfa drugs (a) Viagra®, (b) Agenerase®, Celebrex® (Aslan 2017)

Reasons such as the rapid spread of the HIV virus, the emergence of new pathogenic bacteria such as SARS, and the resistance of bacteria to existing drugs (MDR Mycobacterium tuberculosis and "vancomycin" resistant Staphylococcus aureus) have brought infectious diseases to a level that threatens human health. In addition, the use of bacteria such as Yersinia pestis and Bacillus anthracis for bioterrorism has necessitated new studies on infectious diseases. Studies on this subject proceed in two ways: both synthesizing new drugs with antimicrobial activity and detecting new target enzymes in pathogenic bacteria (Greenfield and Bronze 2003, Babaoglu *et al.* 2004).

In higher organisms, including vertebrates, CA I, II, and IV isoenzymes are responsible for maintaining acid-base balance and respiration (Esbaugh and Tufts 2006, Maren 1967). CA II isoenzyme provides differentiation of osteoclast and plays a role in bone development (Tarun *et al.* 2003). CA isoenzymes are also involved in the secretion of electrolytes from tissues and organs, and in the sense of smell and taste. In this way, the gastrointestinal tract is protected from very high or very low pH conditions (Esbaugh and Tufts 2006, Supuran *et al.* 2003). Some isoenzymes, such as CAV, are involved in the intracellular signal transduction process (insulin secretion from the β cells of the pancreas). Isoenzymes II and V provide bicarbonate ions for gluconeogenesis.

They also play a role in the de-novo biosynthesis of fatty acids and the synthesis of pyrimidine bases. In recent studies , it has been determined that IX, XII, CARP VIII isoenzymes are found in excess in tumors (Leppilampi 2006).

he most potent organic inhibitors of carbonic anhydrase are aromatic and heteroaromatic sulfonamides. Sulfonamides have the chemical structure $R\text{-}SO_2NH_2$. where R is usually aromatic or heteroaromatic ring systems. Ki constants for CA-II range from 10^{-5} to10^{-10}.

$R\text{-}SO_2NH_2 \rightarrow R\text{-}SO_2NH^- + H^+$

One of the most remarkable characteristics is of sulfonamides is that they can easily acquire an ionic structure. This characteristic is crucial for the suppression of the CA enzyme. In addition to this hydrophilic region, sulfonamides also have aromatic and heteroaromatic hydrophobic regions. The interaction of sulfonamides with the enzyme primarily occurs by ionic bonding of the N atom in the $R\text{-}SO_2NH^-$ compound to the Zn^{+2} ion in the active site of the CA enzyme. It is then completed by hydrophobic contacts linking the inhibitors to the enzyme. The combination of these two actions results in high sulfonamide binding to the CA enzyme. Indeed, because only hydrophobic interactions occur during the binding of substituted or alky sulfonamides to the enzyme, they have less inhibitory characteristics than those with aromatic and heterocyclic side groups (Özensoy 2002).

2. LITERATURE REVIEW

2.1 Electromagnetic Wave

Nonmechanical waves that transfer at the (velocity) of light are known as electromagnetic-waves (in vacuum).Light allows us to view the world around us. The Sun's light is one of the sources of energy that we humans use to thrive on our planet. The need for light in comprehending the structure is critical. The qualities of different objects range from atoms to the universe. Even human eyes are unable to see objects in the absence of light.What is light? This conundrum kept many physicists up until the mid-nineteenth century. Previously, numerous scientists believed that electromagnetism and optics were two distinct areas of physics. However, according the jop of Physicist J.C. Maxwell, who truly high lighted the connotation of light with his tehoretical expectations, light is an electromagnetic-waves that flows at a velocity of "3 x 10^8 m/s" (in empty space or vacuum).

Light was later revealed to be merely a minor component of the electromagnetic spectrum, which covers it all from gamma-rays to radio-waves present day digital age, mobile phones (Figure 2.1 (a)) have a rising impact on our everyday life. Being more efficient way of transferring data the one area the other. It utilises the premise because electromagnetic waves make up light. In hospitals, X-rays, which are also electromagnetic waves, are utilized to pinpoint the location of a bone fracture. This may be done using X-rays, which are also electromagnetic waves, as illustrated in (Figure 2.1 (b)) . Microwave ovens are used for cooking. Microwaves are also electromagnetic-waves. Electromagnetic waves have several uses in engineering, medicine (for instance, LASER surgery), defense (like RADAR signals, for instance), also basics scientific study.The fundamentals of electromagnetic-waves (Vainshtein 1988).

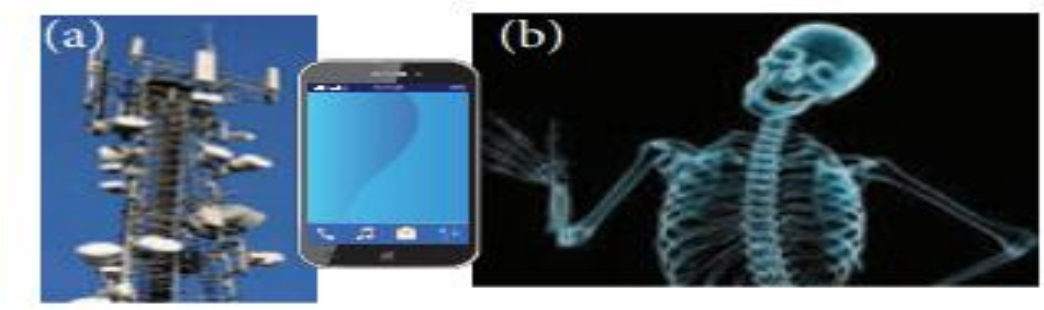

Figure 2.1 (A) mobile device and cell tower (b) A human being's X-ray radiograph (Vainshtein 1988)

Properties of Electromagnetic-Waves

1. Every accelerating charge produces electromagnetic-waves.

2. Electromagnetic-waves propagate without the use of any medium.

3. Electromagnetic-waves are by definition transverse. This demonstrates that the oscillating electric-field, oscillating magnetic-field, and propagation vector, which specifies the propagation direction, are all perpendicular to one another. The propagation path is along the x axis, whereas the electric and magnetic-fields are along the y and z axes, respectively (Figure 2.2) depicts this.

4. Electromagnetic-waves transfer in a straight line. In a vacuum or open space, a speed equal to the velocity of light

C= $\frac{1}{\sqrt{\varepsilon 0\ \mu o}}$ = 3 x 10^8 $\frac{m}{s}$, Where ε_0 empty space or vacuum permittivity and (μ_o) is the free space or vacuum permeability.

5. The speed of an electromagnetic-wave in a material with permittivity and permeability is smaller than the velocity in open space or vacuum, that is, that is, v < c

In a medium of refractive index, $\mu = \frac{c}{v} = \frac{\frac{1}{\sqrt{\varepsilon 0\ \mu o}}}{\frac{1}{\sqrt{\varepsilon \mu}}} \Rightarrow \mu = \sqrt{\varepsilon_r\ \mu_r}$, where ε_r is

the medium's relative permittivity (also known as dielectric constant), and μ_r the medium's relative permeability.

6. An electric or magnetic field cannot deflect electromagnetic-waves.

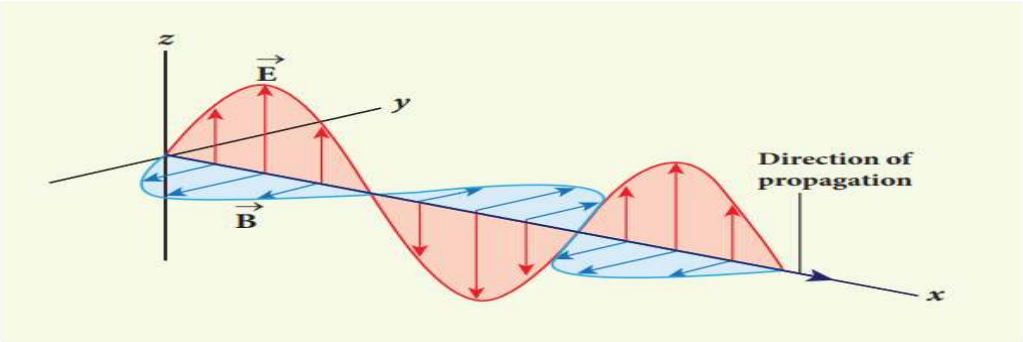

Figure 2.2 Electromagnetic-waves transverse wave (Vainshtein 1988)

7. Electromagnetic-waves can interfere, diffract, and be polarized.

8. An electromagnetic-wave moving in a vacuum or empty space has an energy density (energy per unit volume).

9 . The electromagnetic-wave's average energy-density, $(u) = \frac{1}{2}\varepsilon_0 E^2 = \frac{1}{2}\frac{1}{\mu_o} B^2$.

10 . The intensity is the amount of energy moving across a given area in a given length of time, perpendicular to the course of an electromagnetic wave. Intensity, $I = (u)c$ or

$$I = \frac{\text{total electromagneticenergy (U)}}{\text{Surfacearea (A)X time(t)}} = \frac{\text{Power (P)}}{\text{Surfacearea (A)}}$$

Note : For a point source, $I = \frac{P}{4\pi r^2} \Rightarrow I \alpha \frac{I}{r^2}$

For a line source, $I \alpha \frac{I}{r}$

11. Electromagnetic-waves, such as other waves, convey energy and motion. The linear momentum of an electromagnetic-wave with energy U propagating at speed c is is given by $= \frac{\text{Energy}}{\text{Speed}} = \frac{U}{C}$. Radiation pressure is the force produced by a unit area of a surface being struck by an electromagnetic wave.

12 . Sources of electromagnetic waves.

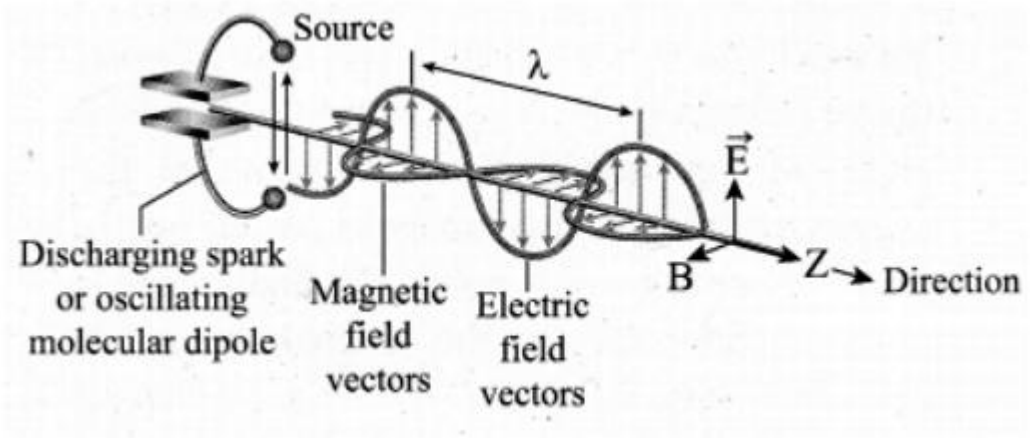

Figure 2.3 Oscillating charges - sources of electromagnetic waves (Vainshtein 1988)

Only an electric-field is produced by any stationary source charge. When a charge moves at a constant speed, it produces a continuous current, which creates a magnetic-field (solely spatially dependent, not time-dependent) surrounding the conductor. When a charged particle accelerates, it creates a magnetic-field in addition to an electric-field. Electric and magnetic fields are also timevarying. The propagation path is perpendicular to the plane containing the vectors of the electric and magnetic fields. because electromagnetic waves are transverse waves. Because every oscillatory motion is also an accelerating motion, electromagnetic-waves are produced If a charge is fluctuating (oscillating molecular dipole) around its mean location, as illustrated in Figure 2.3.

13 . If an electromagnetic-wave is totally absorbed by a physical surface, the energy given is U and $p = \frac{U}{C}$ is the amount of momentum transferred to the surface (Vainshtein 1988).

Visible light is limited to a wave-length range of 420–680 nm (Laufer 1996, Bradt 2004).

2.1.1 Radio-waves

Radio-waves have a frequency range of 300 (GHz) to 30 (Hz). 300 GHz has a wave-length of 1 mm (less than a rice grain), (Altgelt 2005). while 30 Hz has a wave-length of

(10,000) km (longer than the Earth's radius). Radio-waves, same other electromagnetic-waves, Moving at the 3 $x10^8$ m / s in a vacuum, but at a slightly faster rate in the Earth's atmosphere. Senders create artificial radio-waves, which radio receivers receive via antennas. Radio-waves are employed in both stationary and mobile applications. Antennas, television, radar, radios, data satellites, cell phones, and a variety of other applications are all possible. Conversely, shorter waves may return to the surface beyond the horizon after bouncing off the ionosphere (sky waves) (Ellingson 2016).

James Clerk Maxwell, a Scottish mathematical scientist, predicted radio waves for the first time in 1867 (Harman 1998).

2.1.2 Micro-waves

Micro-waves are a form of electromagnetic-radiation with wave-lengths that range from 1 meter to 1 millimeter and frequencies that range from 300 MHz to 300 GHz. (Hitchcock 2004). The frequency regions of micro-waves are described differently by different sources; the following general term covers both Ultra high frequency and Extremely high frequency (mm wave) bands. A relatively joint term engineering of radio frequency is the band between (one anto one hundred GHz). wave-lengths from 0.3 m to 3 mm . In all conditions, micro-waves cover the whole very high frequency band (three to thirty GHz, or ten to one cm) (Jones *et al.* 2013).

2.1.3 Infrared (IR)

Infrared (IR), sometimes known as "infrared light," is a kind of electro-magnetic radiation (EMR) with longer wave-lengths than visible-light. As a result, it cannot be seen with the naked eye. IR wavelengths are widely assumed to span from around 0.001 m ($3x10^2$ GHz) to the theoretical the visible spectrum's reddest part. This is around 7 $x10^2$ nm (43 $x10^1$ terahertz) (Liew 2006). (However, longer infrared wavelengths (thirty µm- a hundred µm) are often called terahertz radiation (Rogalski 2019). Near-room-temperature black-body radiation is virtually completely infrared. Infrared (IR) is

a kind of electromagnetic-radiation that proliferates momentum and energy with features akin to both a wave and a particle, the photon (Fleming 2008).

Thermal imaging cameras with infrared capabilities are employed in insulated systems to identify heat loss, monitor changes in blood flow in the skin, and diagnose electrical component overheating (Chilton 2014).

The wavelength is oppositely related to frequency v, and is determined by the formula $v = c/\lambda$, where c is the velocity of light. Also, the energy is related to frequency: $E = h v$, where h is Planck's constant. The latter equation demonstrates that the X-ray part of the spectrum contains the most energetic radiation, where the energy may be sufficient to disrupt molecular bonds. On the other hand, Radio frequencies only contain relatively little energy, only enough to generate Nuclear magnetic resonance (NMR) or electron spin resonance (ESR) are the results of nuclear or electronic spin changes within molecules. (Table 2.1) outlines the spectral areas and energy transfers and their kinds detected in each. Several of these zones, especially the infrared, provide crucial info about organic molecule structures. The majority of chemists speak of vibrational infrared radiation portion of the electromagnetic spectrum in terms of a unit termed a wavenumber (k), rather than wavelength, because it occurs in the radiofrequency section of the spectrum (μ or μm) (Donald *et al.* 1979).

Table 2.1 types of energy exchanges in each section of the electromagnetic spectrum (Donald et al. 1979)

Region of Spectrum	Energy Transitions
X-rays	Bond breaking
Ultraviolet/visible	Electronic
Infrared	Vibrational
Microwave	Rotational
Radiofrequencies	Nuclear spin (nuclear magnetic resonance) Electronic spin (electron spin resonance)

Wavenumbers are measured in reciprocal centimeters (cm^{-1}) and may be readily calculated by multiplying the wavelength in centimeters by the reciprocal. By multiplying a wavenumber K by the speed of light, you may convert it to a frequency V (expressed in centimeters per second) (Donald *et al.* 1979).

$$K(cm^{-1}) = \frac{1}{\lambda\,(CM)} \qquad V(HZ) = K(C) = \frac{C\,(\frac{cm}{sec})}{\lambda\,(cm)}$$

The fact that wavenumbers are exactly proportional to energy is one of the key reasons why chemists choose to use them as units. The vibrational infrared ranges from around 4 $x10^3$ to 4 x 10^2 cm^{-1} in terms of wavenumbers. The wavelengths in this range are 2.5 to 25 μm. We shall only utilize wavenumber units. We use the following relationships to convert wavelengths (μ or μm) to wavenumbers (cm^{-1}):

$$cm^{-1} = \frac{1}{(\mu m)} \text{ x } 10000 \qquad \text{and} \qquad \mu m = \frac{1}{(cm^{-1})} \text{ x } 10000$$

2.1.4 Visible light

It is generated by incandescent substances and emitted by atomically excited gases. The wavelength domain is (4 x 10^{-7} m to 7 x 10^{-7} m), whereas the frequency domain is (7 x 10^{14} Hz to 4 x 10^{14} Hz). interference, diffraction, polarisation, reflection, refraction, interference, and photoelectric effect, and photographic activity are all rules that it obeys. It may be used to investigate molecules' composition, and how electrons are arranged in atoms' exterior shells (Vainshtein 1988).

Gamma-rays, X-rays, micro waves, and radio waves are all forms of light in this sense. The fundamental characteristics of light include intensity, propagation direction, frequency or wave-length spectrum, and polarisation. Its speed in a vacuum is 3 x 10^8 (m/s), one of nature's basic constants (Uzan *et al.* 2008).

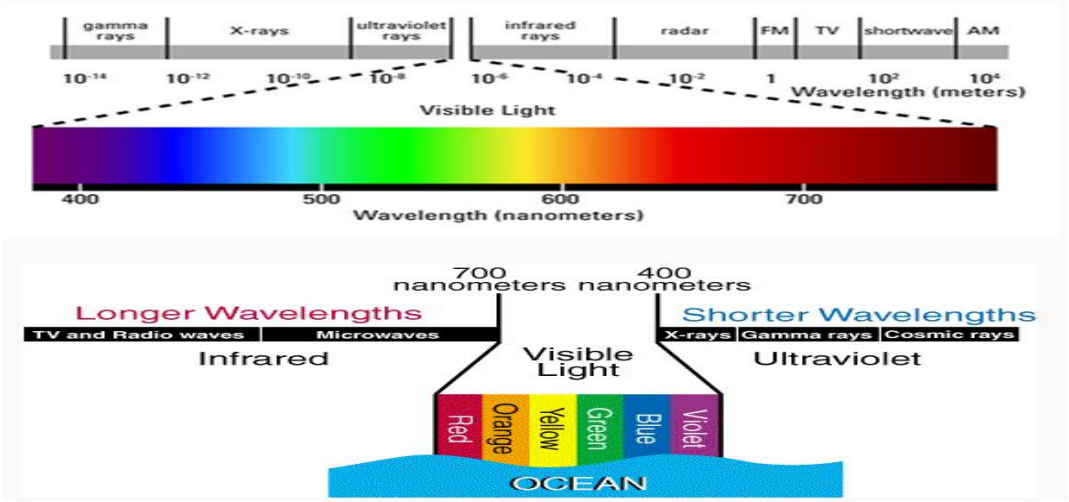

Figure 2.4 Visible Light Electromagnetic Spectrum (EMS 2004)

2.1.5 Ultraviolet (UV)

The Sun, and ionized gases all contribute to its creation. The frequency domain is (5 x 10^{17} Hz to 7 x 10^{14} Hz) , while the wave-length domain is (6 x10^{-10} m to 4 x10^{-7} m). It has a lower penetration rate. It may be absorbed by ozone in the atmosphere and is damaging to the body of a human. It's used to kill bacteria, sterilize surgical equipment, identify invisible writing and finger prints, and investigate molecular structure, among other things (Vainshtein 1988).

Ultraviolet light is the area of the electromagnetics pectrum between X-rays and white spectrum. Air is ionized so powerfully by more intense, shorter wavelength "extreme" UV below 121 nm that it is absorbed before it reaches the earth .Spectrometers and radiometers are used to measure UV radiation. Detectors made of silicon are employed across the spectrum (Haigh 2007). In most terrestrial vertebrates, including humans, ultraviolet radiation (particularly UVB) is responsible for the production of vitamin D (Wacker and Holick 2013).

2.1.6 X-ray

Prior to its discovery in 1895, X-rays were assumed to be a type of inexplicable radiation released by experimental discharge tubes. They were discovered by scientists examining cathode rays, which are powerful electron beams discovered in 1869. Several of the Crookes tubes (created around 1875) very likely released X-rays, as demonstrated by the effects seen by early researchers, as described below. Tubes for Crookes produced free electrons by ionizing the remaining air inside the tube with a high DC voltage ranging from a few thousand volts to 100 keV. When electrons from the cathode impacted the anode or the tube's glass wall, they were propelled to such a high speed that they generated X-rays. Wilhelm Conrad Röntgen was the first researcher suspected of accidentally producing X-rays. He gave a presentation to the Royal Society of London in 1785, explaining the effects of running electrical currents down a partly evacuated glass tube, resulting in an X-ray-like light (Filler 2009). German physicst wilhelm conrad rontgen ,who discovered it on november 18,1895. He gave it the term "X-radiation." (Novelline 1997).

x-ray It's caused by the abrupt slowing of high speed electrons at a high atomicnumber target as well as electronic transitions between atoms' innermost orbits. The frequency domain is (3 $x10^{21}$ Hz to $1x10^{16}$Hz), while the wavelength domain is (10^{-13}m to 10^{-8}m). The penetrating strength of X-rays is greater than that of UV light. X-rays are widely employed in the investigation of internal atomic electron shell configurations as well as crystal formations. It is used to identify fractures, damaged organs, bone and stone development, and the progression of mending bones. It is also used to identify problems, fractures, flaws, and holes in a final metal product (Vainshtein 1988).

2.1.7 Gamma-ray γ

A gamma-ray, often known as gamma-radiation, is a type of penetrating electromagnetic-radiation created by nuclear reactions of nucleons. It is composed of electromagnetic waves with the shortest wavelengths, which are usually shorter than X-rays. At frequencies greater than 30 exahertz (30 x 10^{18}Hz). The energy domain of

gamma-rays generated by radioactive decay ranges from some few (keV) to around 8 (MeV), which corresponds to the usual energy state in long-lived nuclear atoms. Gamma-spectroscopy May be used to identify radionuclides that are decaying by examining their energy spectrum. Very high energy gamma-rays in the 100 to 1000 (TeV) domain have been seen form sources such as the "Cygnus X-3 microquasar". In astronomy, gamma-rays are photon energies more than 100 keV, whereas X-rays are photon energies less than 100 keV. Human health is endangered by ionizing radiation, such as gamma rays. Because of their high penetrating strength, they can injure internal organs and bone marrow. They move through the body fast, unlike alpha and beta rays, and so offer a major radiation protection challenge, needing shielding made of dense materials like lead or concrete. Except for gamma-rays, which are absorbed by 0.53 bar of atmosphere when they enter the atmosphere, the magnetosphere shields Earth from the majority of damaging cosmic radiation. Gamma rays have such small wavelengths that they can only pass between atoms in a detector and cannot be reflected by a mirror (Villard 1900, L'Annunziata 2007).

2.2 Spectroscopy

Spectroscopy is the analysis of the relationship of matter with electromagnetic radiation as a function of the wave length or frequency of the radiation. Spectroscopy is the scientific analysis of color as it pertains to all regions of the electromagnetic-spectrum, especially visible- light. The analysis of the wave-length dependency of visible-light dispersed through prism absorbance by gas-phase materials gave rise to spectroscopy. Matter-waves and acoustic waves are examples of radiant energy, and gravity-waves have recently been connected to spectral characteristics as part of the Laser Interferometric Gravitational Wave Observatory "LIGO". Spectroscopy, especially in the electromagnetic- spectrum, is a basic investigative technique in physics , astronomy, and chemistry, allowing researchers to analyze the composition, electronic structure of matter on an atomic, physical, molecular, and macro scale (Bunker and jensen 2006, Skoog *et al.* 2007). Because the spectrum of molecules and atoms differ, spectroscopic is being used in analytical chemistry and physical . As a result, these spectrum can be utilized to detect, recognize, and measure information on molecules and atoms .

Spectroscopic is used in astronomy and sensing on the ground. Spectro graphs may be found on almost every research telescope. The observed spectrum are used to derive the chemical structure and physical properties of celestial objects (such as their density of elements in a star,temperature, velocity, and black holes and more) (Hungund 2020).

Spectroscopy is the study of how light and other forms of radiation are absorbed and emitted by materials. In a similar way to how a prism divides light into a rainbow of colours, it involves breaking down light (or more particularly electromagnetic radiation) into each of its constituent wavelengths.In actuality, photographic plates and a prism were used to do traditional spectroscopy. Modern spectroscopy projects the light that has been scattered by a diffraction grating onto CCDs (charge-coupled devices), which are comparable to those used in digital cameras. This digital format makes it simple to extract the 2D spectra and alter them to create 1D spectra with a significant quantity of valuable data. The concept of spectroscopy has recently been broadened to encompass the study of particle interactions including interactions between particles like ions, protons, and electrons as a function of impact energy. Spectroscopy is not a specialized or isolated science, but rather a crucial component of several academic fields. It supported early quantum studies of radiation and atomic structure theoretically, but it also has a startling array of practical applications, such as those using X-ray and MRI technologies. We assess the distinct composition and physical characteristics of far-off astral entities through their spectra and wavelength, and it's even used to screen for doping in sports. This technique is called radio-frequency spectroscopy (ATASI 2019).

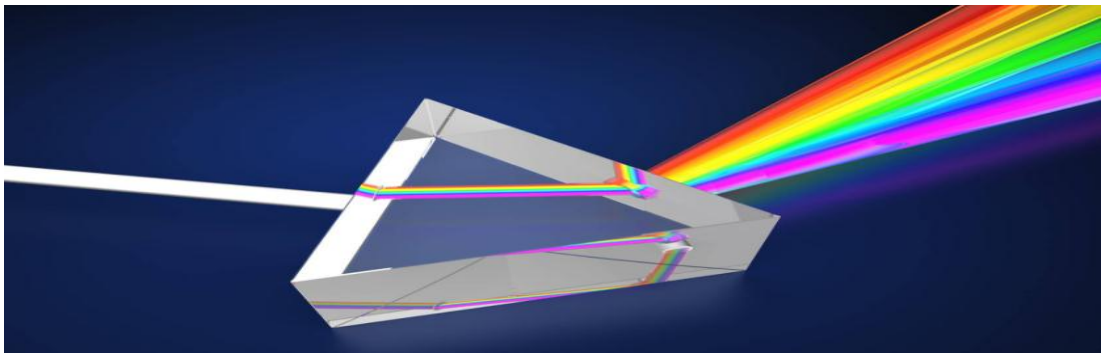

Figure 2.5 A prism analyses white light by scattering it into its component colours as an example of spectroscopy (ATASI 2019)

2.3 Spectroscopic Methods

2.3.1 Ultraviolet–visible spectroscopy

UV spectroscopy, often known as the study of absorption, is called UV-Vis. and reflection spectroscopy in the uv and neighboring portions of the electromagnetic spectrum that are visible. This suggests that it makes use of visible and nearby light. The color of the substances involved is directly affected by their absorption or reflectance in the visual spectrum. Atoms and moleculers undergo electronic transitions in this area of the spectrum. Absorption spectroscopy is similar to fluorescence spectroscopy in that it measures transitions from the ground state to the excited state, whereas fluorescence measures moves from an excited state to a ground state. (Skoog *et al.* 2007).

A method of optical spectroscopy that utilises light in the visible, ultraviolet, and near-infrared wavelengths is known as ultraviolet (UV) spectroscopy. Based on the Beer-Lambert equation, the content of the absorbing substance in the liquid and the route length are exactly proportional to the absorbance of a liquid. Thus, the content of the absorber in a liquid may be determined using UV/VIS spectroscopy for a constant route length. It is necessary to know how quickly absorbance varies with concentration. The analytical technique is based on evaluating the monochromatic light's absorption by colourless substances in the nearly ultraviolet path of the spectrum (200-380nm) (Gandhimathi *et al.* 2012).

2.3.2 Atomic-absorption-spectroscopy

(AAS), Atomic Absorption spectroscopy in both flames and electro - thermal modes, is one of the most effective techniques for determining metal contents in different acid-dissolved specimens (Kalbasi and Mosaddegh 2012). Preconcentration and separation, a sample dissolving are critical phases in many operations, especially when dealing with

low-metal concentrations. AAS was used to determine metals levels in nanomaterials since it is relatively sensitive to (Pd) and (Rh) (Scaccia and Goszczynska 2004).

Clinical metal analysis in biological fluid or tissue like as whole plasma, blood, urine, saliva, brain tissue, liver, hair, and muscle tissue are some of the uses of atomic absorption spectrometry in chemistry (Koirtyohann 1991).

2.3.3 Nuclear magnetic resonance spectroscopy

(NMR) Nuclear magnetic resonance is a spectroscopic technique that organic chemists value even more than infrared spectroscopy. NMR techniques can be used to study a variety of nuclei, but hydrogen and carbon being the most commonly available. While infrared-spectroscopy shows the sorts of functional groups found in a molecule, (NMR) indicates the number of magnetically different atoms of the type under investigation. When hydrogen nucleus (protons) are investigated, for instance , the number of each of the many types of hydrogen nuclei may be determined, as well as information on the nature of each type's immediate surroundings.Carbon nuclei have comparable characteristics that may be identified. The combination of IR and NMR data is typically sufficient to determine the entire structure of an unknown molecule (Donald *et al.* 1979). To examine the local magnetic fields around atomic nuclei, nuclear magnetic resonance spectroscopy, sometimes referred to as NMR spectroscopy or magnetic resonance spectroscopy (MRS), is utilised. The sample is placed in a magnetic field and radio waves are used to excite the sample's nuclei, creating an NMR signal that can be picked up by sensitive radio receivers. The resonance frequency of a molecule is altered by the intramolecular magnetic field around an atom, providing access to details of the molecule's electronic structure and specific functional groups. Therefore, NMR Spectroscopic methods is the best way for identifying mono-molecular organic compounds in contemporary organic chemistry because fields are distinct or very specific to particular substances.

The NMR concept is generally broken down into three steps:

1. Magnetic nuclear spin polarization (alignment) in a constant magnetic field, B_0.

2. A weak magnetic field that is fluctuating, commonly referred to as a radio-frequency (RF) pulse, perturbs this nuclear spin alignment.

3. analysis and detection of electromagnetic waves generated by the sample's nuclei as a result of the disturbance.

NMR is a tool used by biochemists to identify complicated proteins compounds in the same way. In addition to identifying them, Molecular structure, kinetics, reaction state, and chemical environment may all be precisely determined using NMR spectroscopy. The most often utilised types of NMR spectroscopy are proton and carbon^{-13}, however it may be used to any substance having spin-containing nuclei. NMR spectra are unique, well-resolved, analytically tractable, and often quite predictable for small-molecule molecules. Even identical functional groups with different neighbouring substituents can provide various signals, allowing the distinction of different functional groups to be made clearly. NMR has virtually replaced traditional wet chemistry methods for identification, such as reagents for colour or conventional chromatography. One downside is that a substantial amount of purified material, 2–50 mg, is required, albeit this can be recovered by a workup. due to NMR examination of solids needs a specialised magic angle spinning apparatus and might not offer spectra with the same level of resolution, the sample should preferably be dissolved in a solvent. NMR's timeframe is relatively long, making it unsuitable for viewing quick processes, as it only produces an average spectrum. Despite the fact that NMR is fundamentally insensitive, even if sensitivity rises at higher frequencies, and despite the fact that enormous amounts of contaminants can be seen on an NMR spectrum, there are superior methods for detecting impurities (Teng 2012).

2.3.4 Mass-spectrometry

The mass to charge ratio of ions is determined using mass spectrometry, an analytical method. The data is shown as a mass spectrum, which is a plot of intensity vs mass to charge ratio. Mass-spectrometry is utilized in a domain of areas and may be applied to

both pure materials and mixtures including them. The ratio of mass to charge is shown as a function of the ion signal in a mass-spectrum. The purpose of these spectra is to identify a sample's element or isotope composition, particle and molecule masses, and In the composition or chemical make-up of molecules and other compounds, A sample, which might be either a solid, liquid, or gas, is ionised in a classic MS technique by being bombarded with an electron stream, for example. This causes a few of the sample's molecules to either without fragmentation, acquire a positive charge or to fragment into positively charged shards. Then, by accelerating and exposing When these ions (fragments) are exposed to an electric or magnetic field, they are sorted according to their mass to charge ratio. Ions with identical mass to charge ratios exhibit similar deflection. A device that can detect charged atoms and molecules, like an electron multiplier, is used to detect the ions. The data are shown as spectra of detected ion signal strength vs mass to charge ratio. To identify the sample's atoms or molecules, a distinctive fragmentation pattern or comparing known masses (e.g., a full molecule) to recognized masses can be employed (Sparkman 2000).

2.3.5 X-ray spectroscopy

X-ray spectroscopy is a catch-all name for a variety of spectroscopic methods that use X-ray excitation to describe a substance. An electron in an atom's inner shell is excited by the energy of a photon, which causes it to leap to a higher energy level. When you return to a lower energy-level, During excitation, energy is absorbed and released as a photon with the element's characteristic wavelength (there can be several distinct wavelengths for each element). The limit of X-ray emission provides qualitative informations about the sample's original composition. When the spectrum of a sample is compared to the spectra Quantifiable results are derived from samples of known composition. a stream of charged particles with high energy, such as electrons (in an electron microscope, for instance), protons, or x-rays, can excite atoms. With the exception of carbon, these techniques allow for the analysis of elements throughout the whole periodic table (hydrogen, helium, lithium). An electron beam excites X-rays in an electron microscope. Atomic X-ray energy-dispersive spectroscopy and wavelength-dispersive X-ray spectroscopy are the two major approaches for investigating

characteristic X-ray spectroscopy. The corresponding atomic structure is recorded in the X-ray transmission via the electrical image and Compton effects (Agarwal 2013).

2.3.6 Raman spectroscopy

A spectroscopic technique is Raman spectroscopy for determining the modes of vibration of molecules, as well as rotation and additional low-frequency modes of system. In chemistry, Raman spectroscopy is often used to establish a molecular fingerprint that can be used to identify substances. Photon inelastic scattering, often known as Raman scattering, underpins Raman spectroscopy. A monochromatic light source is used, often a laser in the visible, near IR , or near uv spectrum. X-rays, on the other hand, can be employed. The energy of laser photons is changed up or down when they interact with molecules, vibrational modes, or other system excitations. The energy shift reveals informations With regards to the vibrational modes of the system. IR-Spectroscopy frequently provides equivalent but complementary data. To expose a sample, a laser beam is frequently utilized. A lens absorbs electromagnetic radiation from a light source and routes it through a monochromator. A notch filter, edge pass filter, or band pass filter filters away elasticity radiation energy at the laser line wavelength (Rayleigh scatter), and the remaining collected light is distributed onto a detector. Because spontaneously Raman scattering is sometimes feeble, differentiating the weakly in elastically scattered light from the robust Rayleigh scattered laser light has been a major challenge in getting Raman spectra for many years (referred to as "laser rejection") (Graves and Gardiner 1989) Wavenumbers, which have inverse length units, are frequently used to express Raman shifts since this value is directly related to energy. The Raman spectrum's spectral wavelength and wavenumbers of shift may be converted using the formula below: $\Delta\tilde{\nu}\,(\,\mathrm{cm}^{-1}\,) = (\frac{1}{\lambda 0} - \frac{1}{\lambda 1})$

In most circumstances, the unit used to denote wavenumber in Raman spectra is inverse centimetres (cm^{-1}). where is the Raman shift expressed in wavenumber, λ_0 is the excitation wavelength, and λ_1 is the wavelength of the Raman spectrum. Because wavelength is frequently formulated in (nm).

$$\Delta\tilde{\nu}\ (\ cm^{-1}\ ) = (\ \frac{1}{\lambda 0\ (nm)} - \frac{1}{\lambda 1\ (nm)}\ )\ \ x\ \frac{(\ 10^{7}\ \ nm)}{(cm)}\ .$$

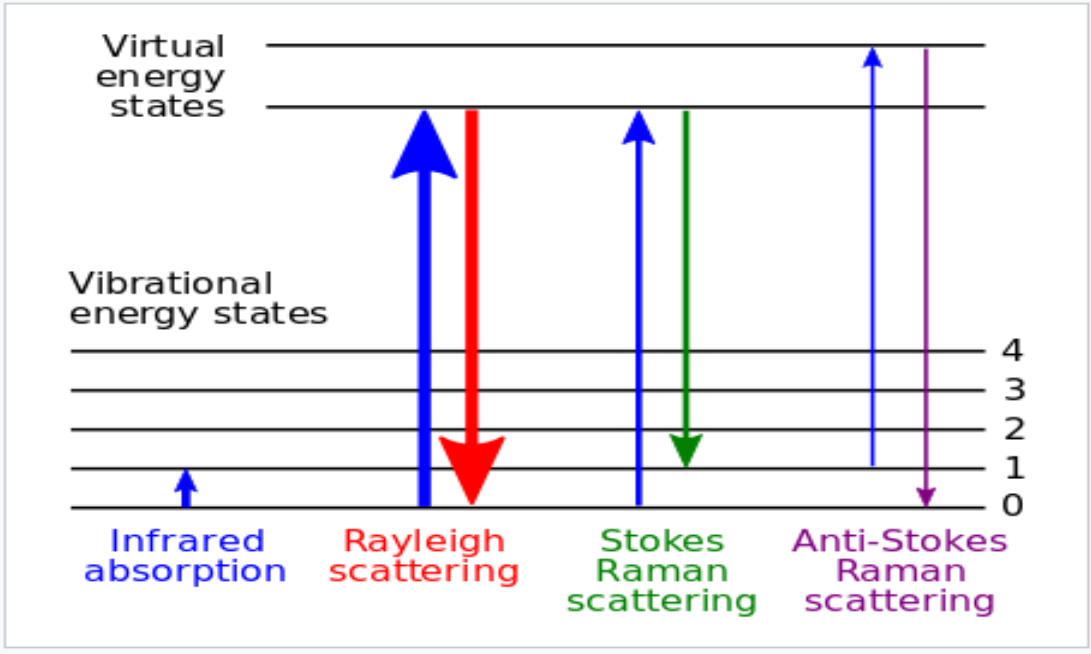

Figure 2.6 Energy-level diagram displaying the Raman Spectra states (Graves and Gardiner 1989)

2.3.7 Infrared spectroscopy

The study of how infrared light interacts with materials through absorption, emission, or reflection is known as infrared spectroscopy (also known as IR spectroscopy or vibrational spectroscopy). Chemical compounds or functional groups in their solid, liquid, or gaseous phases are examined and identified using this method. It may be applied to distinguish and validate known and unknow samples as well as describe innovative materials. An infrared spectrometer, also known as a spectrophotometer, is a piece of equipment used in infrared spectroscopy, which produces an infrared spectrum. An IR spectrum may be represented by a graph with infrared light transmittance (or absorbance) on the vertical axis and frequency or wavelength on the horizontal axis. Infrared spectra typically utilize reciprocal centimeters (also known as wave numbers) with the sign cm^{-1} . IR wavelengths are generally expressed in micrometers (previously "microns") with the symbol µm, which is reciprocally connected to wave numbers. Based on how closely they relate to the visible spectrum, the electromagnetic spectrum's

near-infrared, mid-infrared, and far-infrared regions are typically divided into three groups. Near-IR light with a wave-length of 14 x 10^3- 4 x 10^3 cm^{-1} (7x10^{-1} – 25 x10^{-1} μm) can stimulate molecular vibrations that are overtone or in combination. The mid-infrared, which domains from 4 x10^3 to 4 x10^2 cm^{-1} (2.5-25μm), is commonly employed to investigate basic vibrations and their accompanying rotational vibrational structure. The far-infrared has a low energy range of 4 x10^2 to 1 x10^1 cm^{-1} (25-1x10^3 μm) and can be utilized for low frequency vibrations and rotational spectroscopy. The terahertz zone, which extends from 2 to 130 cm^{-1} and is next to the microwave region, may be used to study vibrations between molecules. The designations and names of these subregions are only conventions according to chemical or electromagnetic characteristics of the subregions (Zeitler *et al.*2007).

Infrared spectroscopy makes use of because molecules may absorb frequencies that are unique to their structure. This absorbing take place at resonance frequencies, which means that the radiation's absorbed frequency corresponds to the "vibrational frequency". The shapes masses of the atoms, surfaces of molecular potential energy, and the accompanying vibronic coupling all have an effect on the energies. The normal modes are connected to the resonant frequencies. of vibration corresponds to the electronic ground state of molecules. In the Born-Oppenheimer and harmonic approximations, potential energy surface that is, when the matching molecular Hamiltonian A harmonic oscillator at the equilibrium molecular geometry can come close to the ground state of electronics. The resonance can include frequencies linked to the bond strength and the mass of the atoms at either end of the bond. As a result, the vibrations' frequency is linked to a certain conventional bond type and mode of motion (Atkins and de Paula 2009).

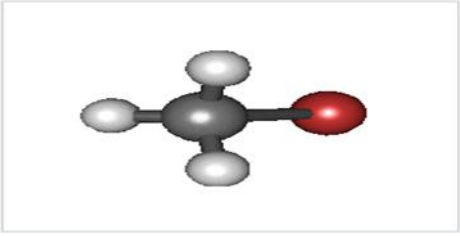

Figure 2.7 Bromomethane's (C-H bonds) symmetric stretch-compress mode in 3D animation (Atkins and de Paula 2009, Schrader 1995)

The number of vibrational modes An oscillatory mode in a sample must be connected with variations in the dipole moment in order to be “IR active”. The rule just needs a change in dipole moment, so a permanent dipole isn't required (Atkins and de Paula 2009). A molecular can vibrate in a number of different ways, each of which is known as a "vibrational mode." Linear molecules contain 3N-5 levels of stretching vibrations, while nonlinear molecules with N atoms have 3N-6 levels of stretching vibrations (also known as degrees of freedom for vibrations). For example, the non-linear molecule H_2O has 3 x 3 – 6 = 3 levels modes or freedoms of vibration. The sole link and vibrational band in simple diatomic molecules is one. Whenever a molecular, such as N^2, is symmetrical, the band shows only in the Raman-spectrum and not in the IR spectrum. Asymmetrical diatomic molecules such as CO are absorbed by the infrared spectrum. Because more complex compounds contain more bonds, their vibrational spectra are also more complicated, resulting in more peaks in the IR spectra of large molecules. The atoms in the CH_2X_2 group, which can be additional atoms and is often found in organic compounds, have nine distinct vibrational modes. There are six of these vibrations that just the CH_2 component: two stretching modes (υ): symmetric (υs) and antisymmetric (υas); as well as four bending styles, as indicated below: Rocking (ρ), Scissoring (δ), Wagging (ω), Twisting (τ). Structures without the two extra X groups possess fewer modes since certain modes are determined by exact linkages to the other linked groups.The wagging, rocking,and twisting modes, for example, need not exist in water because such movements of the hydrogen atoms suggest simple rotations of the molecular chain instead of vibrations inside it. In increasingly complex compounds, out of plane (γ) vibrational modes can be identified (Schrader 1995).

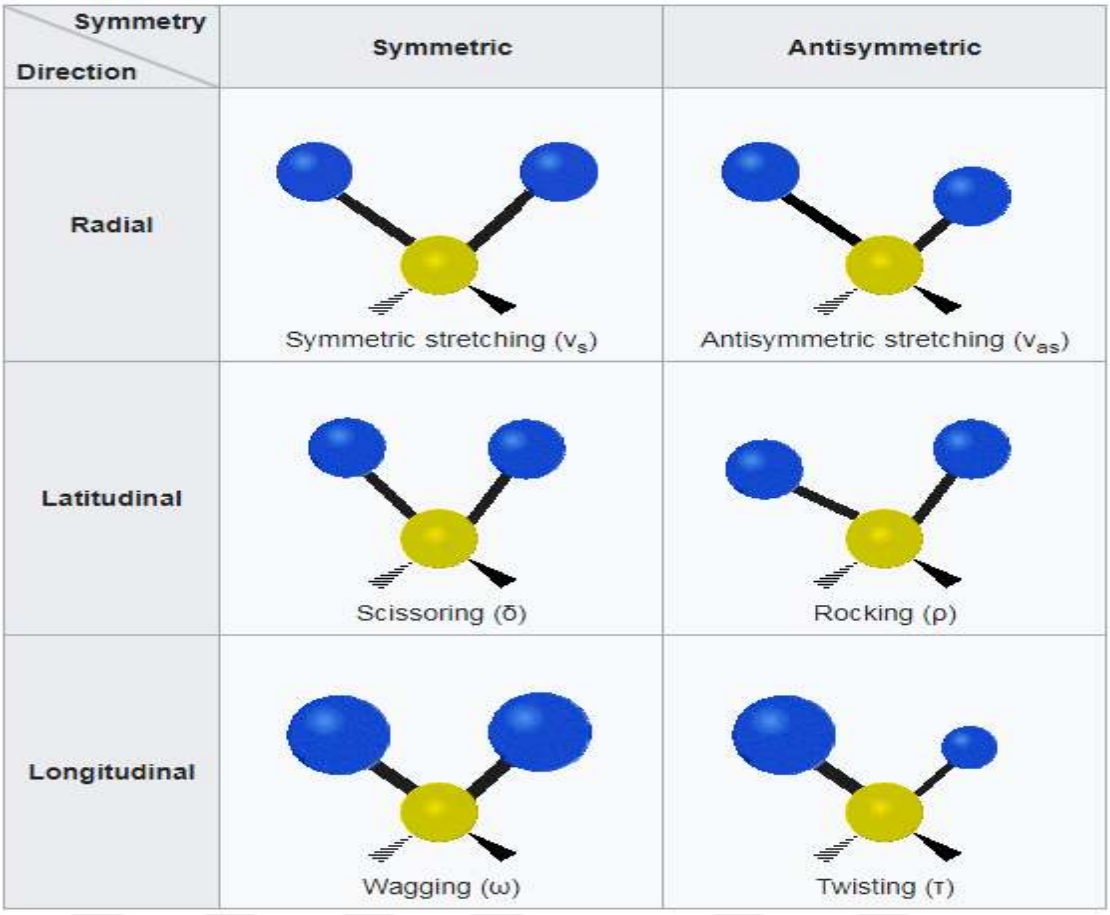

Figure 2.8 Although necessary to balance the overall movements of the molecule, the "recoil" of the C atoms, which is not depicted in these figures, is much smaller than the movements of the lighter H atoms (Atkins and de Paula 2009, Schrader 1995)

2.4 Molecular Vibration Types

A molecule's centre of gravity remains fixed but its atoms move periodically relative to one another in a process known as molecular vibration. The wavenumbers range from (3×10^2 to 3×10^3 cm^{-1}), and the wavelengths range from (3×10^1 to 3 μm), with the average vibration frequencies ranging from less then 10^{13} Hz to roughly 10^{14} Hz. Molecular polyatomic vibrations systems are explained in terms of conventional modes, which are self-contained of one another. The molecule's various parts vibrate at same time for each normal mode. N-atom nonlinear molecules have 3N-6 normal vibration modes while a linear molecule has 3N-5 due of rotation, modes along the molecule plane cannot be seen (Landau and Lifshitz 1976). A molecule with two atoms could

only stretch or squeeze one link, hence it only has one regularly held of vibration. The vibration of a molecular is triggered when a molecule takes in energy, E, that matches the frequency of the vibrations, v, according with equation E = hv, where (h) is the constant of Planck. A basic vibration is produced when a molecule in its initial state absorbs one of these quantums of energy (Hollas 1996, Banwell *et al.*1994).

2.4.1 Stretching vibrations

The tension vibration is connected to the distance between the two atoms, which moves around the bond axis of the atoms. Tensile vibration has a greater frequency than bending vibration (Al-Sammarraie 2021). vibrations that stretch cause the space separating two atoms to expand or decrease while keeping the atoms on the same bond axis. There really are 2 kinds of stretching vibrations: (Ng and Simmons 1999)

2.4.1.1 Symmetrical stretching

In this mode of vibration, atoms move in the same direction as the common bond axis or central atom (Figure 2.9).

2.4.1.2 Asymmetrical stretching

One atom moves closer to the common atom during this vibration while the other moves away from it (Figure 2.9).

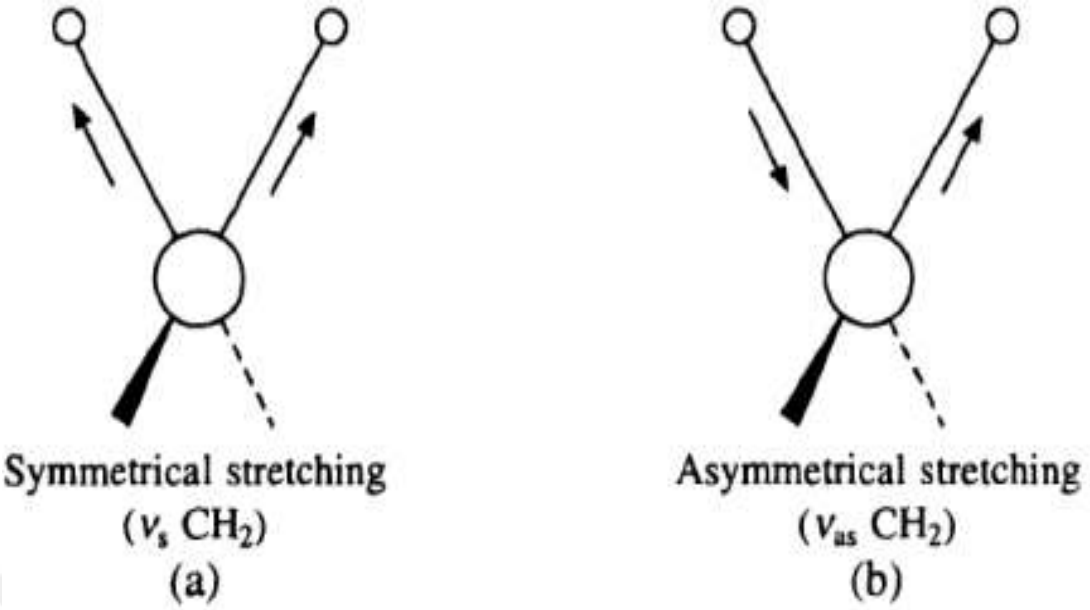

Figure 2.9 CH_2 group stretching vibrations (ν CH_2) (Ng and Simmons 1999)

2.4.2 Bending-vibrations (Deformations) (δ)

The atoms' locations relative to their initial bond axes vary during such oscillations.Four categories of bending vibrations exist.

2.4.2.1 Scissoring(δs)

With a shift in both their bond axes and the bond angle they establish with the center atom, atoms move in the opposite direction during this mode of vibration (Figure 2.10 (a)).

2.4.2.2 Rocking vibration (ρ)

Rocking. With a shift in their bond axes, atoms move in the same direction throughout this vibration (Figure 2.10 (b)) In-plane bendings include scissoring and rocking.

2.4.2.3 Wagging vibration (ω)

According to the common atom, In this vibration, 2 atoms simultaneously move above and below the plane (Figure 2.10 (c)).

2.4.2.4 Twisting (t)

With regard to the common atom, one of the atoms goes up and the other moves down in this mode of vibration (Figure 2.10 (d)).

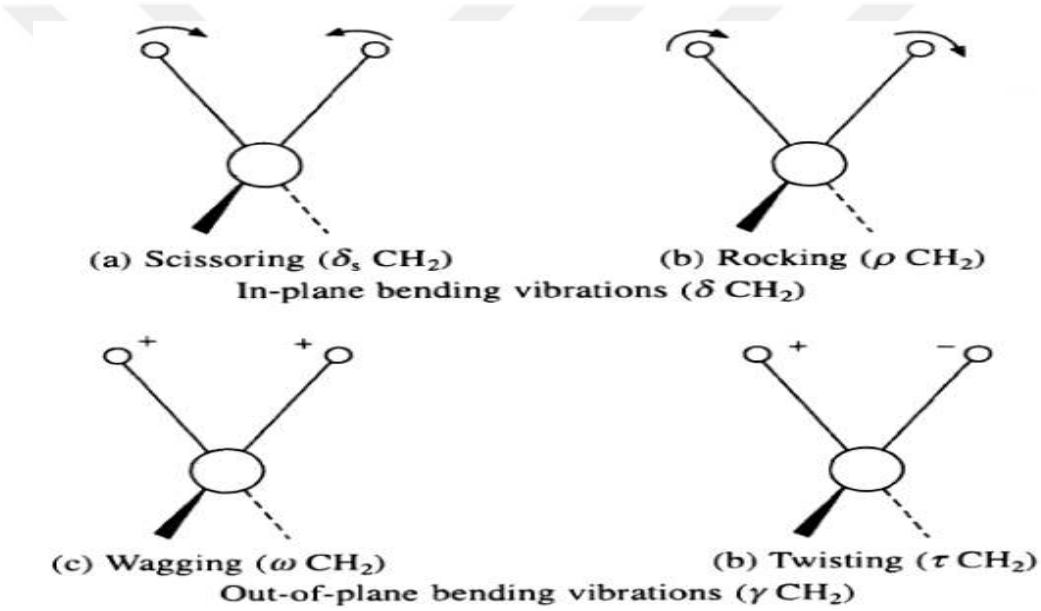

Figure 2.10 A CH_2 group's bending vibrations (deformations) (+ and -signs indicate motions perpendicular to the paper's plane) (Ng and Simmons 1999)

2.4.3 Out of plane bending

In molecules forming a closed circle, out-of-plane angle bending, also known as the action of withdrawing a plane by atom motion, is widespread. Due to the formal structure of the movement, this pulse is represented as a "umbrella vibration" and is denoted by (γ) (Al-Sammarraie 2021).

Figure 2.10 Out of plane bending (γ) (Al-Sammarraie 2021)

2.4.4 Torsion vibration

Torsion movement is the periodic deformation of the bond or angle to change the angle between the two planes. The out-of-plane vibration movement characterized by torsional vibration is referred to as torsional vibration (Al-Sammarraie 2021).

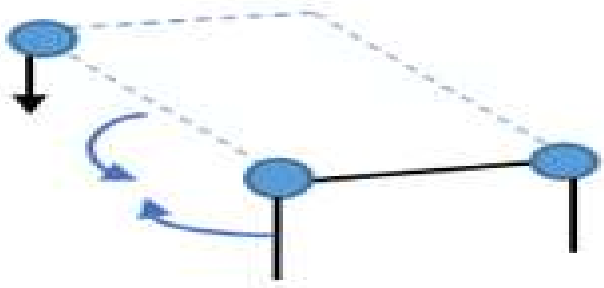

Figure 2.11 Torsion vibration (τ) (Al-Sammarraie 2021)

2.5 Electronic Construction Methods

Electronic structure methods, unlike molecular mechanics methods, classical physics uses quantum mechanics instead. Such methods use the energy of molecules and others to determine many of their properties by solving the Schrödinger equation. But Schrodinger The exact and complete solution of the equation for large molecules is yet to be found. While it is not possible, these methods do some approximations for large molecules. Find the approximate solution to this equation. As a result, for very large molecules, Such methods may not always give the correct result. semi-empirical Although it is divided into two groups as ab-initio and ab-initio methods, the density has

been increased recently. Functional methods (Density functional theory-DFT) are used extensively as a third group (Foresman and Frisch 1996, Dorsett and White 2000).

2.5.1 Molecular mechanics methods

These approaches are classified into several categories and essentially describe the structures of molecules. and is used to specify its attributes. Quantum mechanics is used to determine the characteristics of molecules. It uses classical physics rather than mechanics. Such approaches are not concerned with electrons; rather, they consider nucleon interactions and compute on that basis. Such procedures are frequently related to proteins and polymers. Polymers, for example, are big molecules with extremely high molecular weights that are frequently studied. utilized in some way. Because molecular mechanical methods are not concerned with electrons, problems involving electronic effects cannot be investigated using these approaches. However, they indirectly compute electronic effects, and issues with no electronic effects can also be estimated (Foresman and Frisch 1996).

Molecular modeling comprises all theoretical and computational approaches for modeling or simulating the behavior of molecules (Leach 2001). The approaches are used to explore molecular systems ranging from tiny chemical processes to massive assemblages of materials and biological molecules in the disciplines of materials science, computational biology, computational chemistry, and drug design. The most basic calculations may be done by hand, but computers are essential for molecular modeling of any usefully large system. The atomistic level depiction of molecular systems is a property shared by molecular modeling approaches. This might involve considering the smallest individual units are atoms (a the use of molecular mechanics) or formally modeling protons and neutrons with their quarks, antiquarks, and gluons, and electrons with their photons (a quantum chemistry approach).

2.5.2 Semi-experimental methods

Semi-experimental approaches are used to optimize big molecules and various methods are employed to examine their attributes. These algorithms compute all atom orbitals. They are exclusively concerned with valence electrons and are spherically symmetrical. In HF theory, the approaches neglect the Coulomb and exchange interactions and instead rely on their experimental characteristics. These approaches were discovered through experimental research. Some parameters are used to simplify calculations. If adequate experimental parameters can be found, the Schrödinger equation can be solved using this approach. Good outcomes are conceivable with an approximation solution (Foresman and Frisch 1996, Dorsett and White 2000).

2.5.3 Ab-initio methods

Any ready-made experimental parameters were not employed in the calculations performed with these approaches. These techniques solely perform quantum mechanical computations. laws and the speed of light, Planck's constant, electron and nucleus weights and charges It is done based on the values of certain physical constants. Methods of quasi-experimentation abinitio It is quicker than other approaches and performs admirably on systems with adequate settings. The level is approaching where ab initio approaches outperform quasi-experimental methods. They are expensive, but they are of great quality for the majority of systems evaluated. provide options Ab-initio procedures are quite big, with hundreds of atoms. It is capable of examining structures in a short period of time (Foresman and Frisch 1996, Dorsett and White 2000).

2.6 Quantum Mechanics Equation of Motion: Schrödinger Equation

A quantum-mechanical system's wave function governed by the Schrödinger-equation which is a linear differential calculus (Griffiths 2004). A crucial conclusion in quantum physics was reached, and its discovery represented a watershed moment in the field's evolution. The equation is called after Schrödinger, who developed it in 1925AD and

presented it in 1926 AD , laying the groundwork for his Nobel Prize-winning work in physics in 1933AD (Schrödinger1926).

The Schrödinger-equation, sometimes referred to as Schrödinger's wave equation, is a partial differential equation that uses the wave function to describe the behaviour of quantum mechanical systems. The Schrödinger Equation is used to determine these systems' trajectory, location, and energy (Pochareddy 2019).

$$i\hbar \frac{\partial}{\partial t} \Psi (\vec{r},t) = \left[\frac{-\hbar^2}{2m}\nabla^2 + V(\vec{r},t)\right] \Psi (\vec{r},t) \quad (2.1)$$

2.7 Born–Oppenheimer Approximation

In quantum chemistry, the approximation is commonly used to velocity up the calculation of molecular wave-function and other characteristics for big molecules. In some circumstances, the premise of separate motion no longer holds, causing the approximation to lose meaning (it is called to "break down"), yet it is frequently used as a springboard for further sophisticated techniques. To use the BO approximation in molecular spectroscopy implies seeing molecule energy as a sum of separate components, such as: E total = E electronic + E vibrational + E nuclear spin (Born and Oppenheimer 1927).

This terms are of varying magnitudes, and the “nuclear spin energy” is so modest that it is frequently overlooked. Electronic energies (E electronic) are made up of kinetic energies, interelectronic different ones, interatomic repulsions, and electron nuclear attraction, which are commonly used for calculating the electronic structure of molecules. Twelve nuclei and forty-two electrons make up a benzene molecule. The Schrödinger equation, which must be solved to ascertain the energy levels and wave-function of this molecule, is a formula for partial differential eigenvalues in the three-dimensional coordinates of the electrons and nuclei, producing 3 x 12 + 3 x 42 = 36 nuclear + 126 electronic = 162 factors with regard to the wave-function. When solving an eigenvalue equation, the computational complexity, or required computer power,

develops far more quickly than the square of the number of variables. Two smaller, sequential stages can be employed when using the B_O approximation: The electronic Schrödinger-equation is solved for a given location of the nuclei while the nuclei are treated as stable. The 126 electronic variables are then used to solve the associated eigenvalue issue. This electrical computation is then performed for various conceivable nucleus locations, i.e. molecular deformations. This might be done for benzene that used a grid of thirty six potential nuclear location coordinates. The energies electronic on this grid are then linked together to provide nuclei's potential energy surface. This potential is then employed in a second Schrödinger-equation including only the nuclei's 36 coordinates (Cormen 2009).

2.8 Variation method

The variational technique is one method to get approaches to the least energy initial state and ground state, as well as some excited states, in quantum mechanics theory. This makes it possible to calculate approximation wave functions like molecular orbitals (Sommerfeld 2011). The variational concept serves as the foundation for this strategy (Griffiths 1995). The approach entails selecting a "trial wave function" based on one or more factors and determining the parameters of the model that result in the lowest energy expectation value. The wave function created by setting the criterias to these values is a rough estimate of the ground state wave function, and the energy in that state's expectation value is an upper limit on fundamental energy. The variational approach is used by the HartreeFock method, the Ritz method and the density matrix renormalization group.

2.9 Hartree - Fock Method and Self Consistent Field (SCF) Theory

In Hartree Fock theory, which was initially formulated for free atoms (Slater 1960) , the system's ground state is represented by assigning each of the N electrons to one group of (IPM) orbitals in ascending energy order. In other words, When the number of electrons approaches equilibrium, each orbital appears twice with the α factor and once with the β factor (i.e., it is "doubly occupied"), and the CI development is truncated after the

terms associated with a single orbital configuration. When non-degenerate, the highest occupied orbital, a unique allocation of this sort occurs, and the system is said to have a closed-shell ground state. However, when degeneracies arise, There are a lot of different orbital configurations that might have the same IPM energy, and the electron configuration is referred to be open-shell. and any orbital configurations that correspond to them should be allowed in .In other words, for an open-shell state, the one-configuration approximation will be of many-determinant type (McWeeny and Sutcliffe 1985). This nomenclature is depicted graphically below for the o atom, using standard orbital naming:

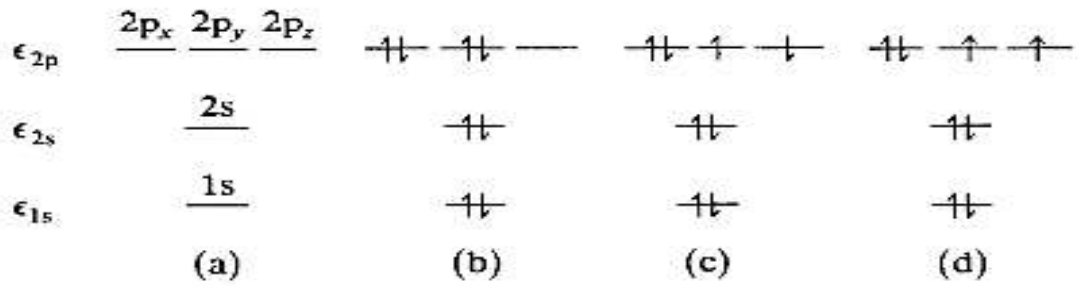

Figure 2.12 The one-configuration approximation of many-determinant type (McWeeny and Sutcliffe 1985)

(a) The oxygen atom's first five orbitals and energy levels.

(b), (c) Two orbital arrangements, $2p_x^2\ 2p_y^2$ and $2p_x^2 2p_y\ 2p_z$ being an arrangement of electrons $ls^2\ 2s^2\ sp^4$.

(d) identical to (c) orbital arrangement, but with a different spin distribution.

Even atoms with open-shell ground states were nearly always addressed with single-determinant wavefunctions in Hartree and others' original work. When the wavefunction is approximated by only one determinant, the name Hartree-Fock (HF) theory (without qualification) is most generally used; we use the word in this meaning, adding qualifications (e.g., "limited," "extended," etc.) where needed. Hartree and Black. (Hartree and Black 1993) presumably did the first multi-determinant calculation for the

3_P state of the oxygen atom. In the vast majority of situations, molecular ground states are reasonably adequately represented by a single configuration of doubly-occupied orbitals, i.e. they are of closed-shell type.

The constant advancement of computer technology and quantum-chemical techniques has increased the number of practical experimental chemists who employ quantum-chemical software programs. These users routinely perform Hartree–Fock (HF) and Kohn–Sham (KS) density-functional theory (DFT) calculations on molecules of sizes and complexity previously unattainable even by the most powerful research programs. This advancement necessitates additional advancements in the automation of the self-consistent field (SCF) process used to optimize the HF and DFT energies, ensuring that convergence may be achieved on a regular basis even for exceedingly complicated molecules (Thøgersen *et al.* 2004).

The SCF process is made up of a series of Roothaan–Hall (RH) repetitions in its original form (Roothaan 1951, Hall 1951). Each cycle begins with the construction of a Fock/KS matrix from the current approximation to the one-electron density matrix, which is then diagonalized to provide a better collection of orbitals and orbital energies, as well as a better density matrix. This increased density matrix is then utilized to generate a new Fock/KS matrix in the next iteration, completing the iteration procedure. However, A RH sequence like this is rare. Only in simple instances do iterations converge. In order to improve convergence, each RH iteration can be extended to include, in addition to the diagonalization step, a stage in which the best density matrix is built in the subspace of the density matrices of the current and prior iterations. In the subsequent RH iteration, the new Fock/KS matrix is constructed using this averaged density matrix rather than the pure density matrix produced from the prior diagonalization (Thøgersen *et al.* 2004).

2.9.1 Slater determinant

A Slater determination is a formula in quantum theory that characterizes the wave equation of a multi fermionic system. It meets anti-symmetry criteria and, as a result,

the Pauli principle, by switching signs when two electrons are exchanged (or other fermions). Only a tiny fraction of all potential fermionic wave equation may be expressed as a singular Slater determinants, but also because of their clarity, they are an important and valuable subset. The Slater determination is derived from a wave equation for a group of electrons, each of which has a spin-orbital $x^{(X)}$wave function, where X specifies the location and spins of a free electron. A wave-function that is (zero) everywhere corresponds to a Slater determination having 2 electrons with the same spin orbital. The Slater determinant was named after John C. Slater, who first proposed it in 1929 as a way to guarantee the anti-symmetry of a many-electron wave function (Slater 1929, Heisenberg 1926, Dirac 1926).

2.10 DFT Methods

The DFT method is called (Density Functional Theory). In the calculation to be made using DFT methods, it is necessary to determine that it should be a function of electron density (Derome 1987, Colthup 1990). DFT methods contain electron correlation effects. However, instead of direct DFT methods, abinitio is usually used. and DFT methods that employ hybrid functions. DFT-hybrid methods are used. The most commonly used method among these methods is B3LYP (Dorsett and White 2000).

Electronic structure's density functional theory (DFT) has had an unprecedented influence about the use of quantum mechanics to intriguing and difficult chemical issues. The number of applications is growing every year, and some of the most recent and important studies address issues in many fields of science and technology, such as the understanding and design of catalytic processes in enzymes and zeolites, electron transport, solar energy harvesting and conversion, drug design, and many others. The story of DFT's success is the pursuit of the exchange correlation functional that makes use of electron density. help elucidate the intricate many-body dynamics taking on within a particle framework.

Despite DFT's widespread use and success, in this overview, we will look at many fields of science and engineering. concentrate on comprehending DFT's existing and

future issues. If the exchange-correlation functional utilized was accurate, DFT accurately describes the quantum nature of matter. It is true that both the success and failure of DFT applications may be attributed to the approximate nature of the exchangecorrelation functional. The potential to build functionals that could offer an adequate description of both molecule geometries and dissociation energy was one of the early DFT advancements that was focused on. The next major challenge for DFT was the requirement to properly predict reaction barrier heights in order to define the kinetics of chemical reactions and to quantify van der Waals interactions. Significant discussion and current research surround the issue of whether DFT can predict the minute energy differences brought on by van der Waals interactions or if further corrections or nonlocal functionals of the density are necessary. Despite being one of the least powerful interactions, it is crucial to comprehend the molecular mechanisms behind several protein-protein and drug-protein interactions.

A fascinating characteristic of DFT is that even the smallest systems can exhibit complexities and problems resembling much bigger and more complicated systems. One example is the concept encapsulated in the commonly used term "strong correlation" as seen in physics literature. Strong correlation, which is based on a determinant of single-particle Kohn-Sham orbitals, refers to a collapse of the single-particle picture, maybe even of DFT itself. It is crucial to keep in mind that this is only a summary of the density functional approximations that are currently in use. strongly coupled systems present the functional with substantial new hurdles (Cohen *et al.* 2012).

2.11 Base Sets

The Hartree-Fock technique or density-functional theory uses a group of functions, known as a basis set, to describe the electronic wave function. This method converts the partial differential equations of the model into algebraic equations that can be efficiently implemented on a computer. By expanding the orbitals $|\psi i\rangle$ inside the "basis set" as a sequential combination of the "basis functions" $|\psi i\rangle \approx \sum_{\mu} c\mu i \, |\psi i\rangle$, where the expansion coefficients $c\mu i$ are determined by $c\mu i = \sum_{\nu} \langle \mu|\nu\rangle\text{-}1 \langle \nu|\psi i\rangle$. the usage of

basis sets is equal to using an approximation of the identity. Atomic orbitals, which provide the approach using a linear combination of atomic orbitals, are the most common choice within the quantum chemistry community. Other options include plane waves, which are frequently utilized within the solid state field, and real-space techniques. Numerical atomic orbitals, Slater-type orbitals, and other atomic orbitals of various sorts can be employed. Given that they enable effective Post-Hartree-Fock method implementation, Gaussian-type orbitals are by far the most popular of the three (Lehtola 2019).

A base set is a mathematical depiction of a molecule's molecular orbitals (Derome 1987). The geometry of the orbitals serves as the foundation for standard basis sets for electronic structure computations. They make use of sequential combination of Gaussian functions. These fundamental functions are sequential combination of gaussian-type functions. Smaller base sets are made up of fewer and smaller base sets, whilst larger base sets are made up of larger and more base sets. As a result, larger base sets require more processing resources. and offer a more precise approximation to the molecular wavefunction.

2.11.1 Minimual base sets

Minimum base sets are the atoms with the fewest number of base functions and constants. It does size computations based on atomic orbitals. The STO-3G base set, for example, is a minimum basis set. Minimum molecular energy base settings are acceptable and proper. Chemical bonds are not normally recommended for prediction, but they can be discovered in basic structures. They give an excellent chance for a qualitative viewpoint (Derome 1987).

2.11.2 Extended basis sets

Similar to the 2.11.1 STOS, the treble and quadruple-zeta basis functions operate with three and four STO_S, respectively. Here too, the traditional trade-off holds true: more

precision results in more costly computations. There are many multiple kinds of extended basis functions, such as n split-valence, n polarised, n diffuse, and n correlation consistent. The terminology for this kind of basis function (with such a Gaussian basis) is N-MPG, and it is used to describe split-valence basis functions. The hyphen designates a split-valence set, and the number N indicates the number of Gaussian functions that characterise inner-shell orbitals. The letters P and M stand for the quantity of Gaussian functions used to match the two orbitals of the valence shell:

1 M is the quantity of Gaussian functions were employed to characterize the smaller orbital.
2 P is the quantity of Gaussian functions were utilized to characterize the bigger orbital (e.g., 6-31G and 3-21G).

Every atomic orbital in a minimal basis function has one basis sets, but that each atomic orbital in a double-ζ basis set has two basis sets. Every atomic orbital has three and four basis functions in a triple-ζ and quadruple-set, respectively. Additionally, higher order basis functions like 5Z and 6Z have been constructed. Numerous basis functions comprised of Gaussian orbitals exist (Figure 2.14). The tiniest of these are referred to as minimum The smallest number of basis functions necessary to represent all of the electrons on each atom makes up many basis sets, and they are typically included in basis sets. On each atom of the largest of them, there may be tens to hundreds of basis sets (Extended Basis Sets 2014).

3-21G	3-21G	3-21G	3-21G* - Polarized	3-21+G - Diffuse functions	3-21+G* - With polarization and diffuse functions
4-21G	4-31G	4-31G	4-31G	4-31G	
6-21G	6-31G	6-31G*	6-31+G*	6-31G(3df, 3pd)	6-311G
6-311G	6-311G*	6-311+G*			

Figure 2.13 Commonly used split-valence basis sets (Extended Basis Sets 2014)

2.11.3 Split valence basis sets

Divided valence basis sets, the orbital changes in size. 3-21G, 6-21G, 6-31G, and basesets such as 6-311G are split valence basesets. Orbitals in these base sets may not change their shape, but their size may change. These base sets are only for valence orbitals. They are distinguished by the number of functions.For example, triple zeta valence basesets such as 6-311G It uses three basic functions. The 6–21G basis set consists of six simple Gaussian functions. an inner-shell atomic orbital with a simplified Gaussian-type function consisting of a gaussian function and an inner valence shell with a simple gaussian function (Derome 1987).

2.11.4 Polarized base sets

These base sets are irregular locations of electrons away from the nucleus. used as a replacement. F-type functions are added by transition metals.2s and 2p carbon atom sp3 hybrid orbitals. Since it is formed with orbitals, it adds a d-type function to the carbon atom. The 6-31G (d) baseset is a polarized baseset. One of the six 6-31G basesets of this baseset, the difference is the six d-type simple gaussian functions added to each heavy atom. Other polarized bases used for medium-sized systems are the 6-31G* and 6-31G** basesets. are set. The base set denoted as 6-31G** is actually the base set of 6-31G (d, p). D-type functions for heavy atoms and p-type functions for hydrogen atoms are added by this base set (Derome 1987).

2.11.5 Diffuse basis sets

Diffuse base sets and functions are generally used for systems where electrons are far from the nucleus, negatively charged ions or other systems, systems with low potential, systems in the excited state, and systems with unpaired electron pairs. These functions indicate that orbitals occupy a larger region when they handle situations. Basesets 6-31+G (d) and 6-31++G (d) are examples of diffuse basesets. Here, the addition of

heavy atoms can perform diffuse functions is +, and the addition to both hydrogen and heavy atoms is ++ (Derome 1987).

2.12 Properties Calculated from Energy

2.12.1 Potential energy surface

Approximation via Born-Oppenheimer is generally considered to function in molecular modeling. This allows the electronics and nuclear movements to be separated; the electrons' considerably lower mass implies that they can quickly respond to any change in nuclear locations. As a result, the energy of a molecular in its ground electronic state can only be thought of as a function of the nuclear coordinate. When some or all of the nuclei shift, the energy typically changes. The altered nuclear locations might emerge from a simple operation like angle bond rotation or from the coordinated movement of a large number of atoms (Leach 2001). The size of the subsequent gain or loss in energy will be determined by the sort of change. For example, it takes around 3 kcal/mol to modify the covalent carbon-carbon bond length in ethane by 0.1 Å from its equilibrium value, but only approximately 0.1 kcal/mol to raise the non-covalent separation between two argon atoms by 1 Å from their lowest energy separation. For tiny isolated molecules, rotation about single bonds results in the least amount of energy change. If we rotate the (carbon-carbon bond in ethane) while holding all of the bond lengths and angles constant, the energy fluctuates in a roughly sinusoidal pattern, as seen in (figure 2.15), with minimal energy at the three staggered conformations. The energy in this scenario may be represented graphically as a function of a single coordinate (i.e., the torsion angle of the carbon-carbon bond), with energy on one axis and the value of the coordinate alnog on the other.

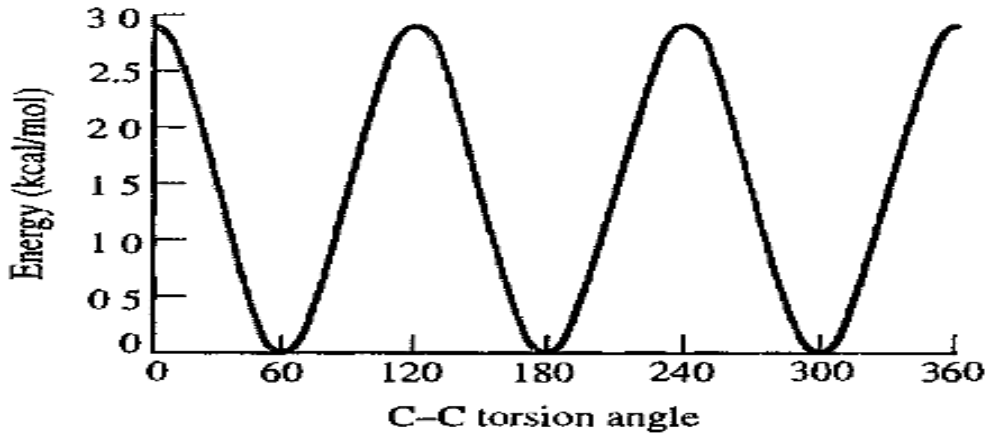

Figure 2.14 Variation in energy with rotation of carbon-carbon bond in ethane (Leach 2001)

Changes in a system's energy can be thought of as movements on a multidimensional "surface," termed the energy surface, where the energy's first derivative is zero in internal or Cartesian coordinates. At a stationary location, all storm forces are zero. One sort of stationary point is a minimal point, which corresponds to a stable structure (Leach 2001).

2.12.2 Geometry optimization

The process of finding stable points in a function is referred to as optimization. Geometry optimization refers to the process of determining the PES minimal energy point and molecular coordinates. During the optimization period, geometry optimization scans the PES beginning from the initial geometry and tries to identify a minimum. The gradient vector given by the Equation (2.2) shown below is computed at each point for this purpose. When optimizing the geometry of a water molecule, for example, one seeks to acquire the The hydrogen-oxygen-hydrogen bond and the lengths of hydrogen-oxygen bonds angles that minimize the forces that would otherwise draw atoms together or push them apart (Energy Minimization 2021).

$$g = \left(\frac{\partial E}{\partial X_1}, \frac{\partial E}{\partial X_2}, \ldots, \frac{\partial E}{\partial X_n}\right) \quad (2.2)$$

Where E is the system's initial energy and x_1, x_2,..., xn are atomic coordinates. The positions that make the gradient vector zero are acquired in the next phase. The minimal energy state corresponds to points where the gradient vector is zero (g=0,0,..., 0). The force constant is determined by the energy with regard second derivative to atomic coordinates. The Hessian matrix, often known as the power constants matrix, is calculated or estimated by the majority of optimization techniques. The curvature of the surface at this point is described by force constants, which aids in determining the following stage. The procedure is completed when the optimization considers that the force is close to zero. A "basis set" is a collection of equations used to characterize an atom's orbital configurations. A linear combination of base functions is used to create molecular orbitals. A predefined base set is used by the majority of quasi-experimental approaches. HF or DFT calculations are dependent on the selection of a base set. In quantum mechanical computations, the "basis set" is just as crucial as the technique. In computations to establish the parameters of a multi-electron system, several molecular integrals are encountered. It is difficult and time-consuming to solve these integrals. As a result, the effectiveness of molecular computations is dependent on selecting the appropriate base set. A decent base set should be able to detect chemical orbitals and make mathematical operations easier. Slater type orbitals and Gaussian type orbitals are the most often employed base sets for atomic and small molecule systems (Jensen 2017).

2.12.3 Gaussian type orbitalis

Gaussian orbitals (sometimes called as Gaussian device, "GTO$_S$", or Gaussians) are atomic orbitals used in the "LCAO" approach to show electrons orbitals in molecules and unique features that rely on these in molecular physics and computerised chemistry (Gill 1994).

Boys first suggested using in the theory of electronic structure, gaussian orbitals in 1950, as opposed to the more useful Slater-type orbitals (Boys 1950). The "Theorem of the Gaussian Product" states that the combination of these two "GTO$_S$" centred on two separate atoms is a limited accumulation of Gaussians centering on a point along the

axis linking them. This is the fundamental justification for using Gaussian basic components in molecular quantum chemistry computations. Four-center integrals may be broken down using this technique into finite averages of two-center integrals, which can subsequently be broken down even further into finite sums of one-center integrals. More than making up for the increased cost associated with the big number of basis functions typically required in a Gaussian computation is the speedup of 4-5 orders of magnitude compared to Slater orbitals. Because integral evaluation is more simpler in the cartesian basis and spherical functions may be written using cartesian functions, many quantum chemistry apps run in a Cartesian Gaussian basis even when spherical Gaussians are required (Schlegel and Frisch 1995).

3. MATERIALS AND METHODS

First, optimization calculation were performed with the DFT/B3LYP method and the 6-311++G(d,p) basis set for the find the lowest energy stable structures of the N^2,N^6-bis-[4-(aminosulfonyl)phenyl]-pyridine-2,6-dicarboxamide compound. The vibrational frequencies of these compound, as well as ^1H and ^{13}C NMR calculations, will next be performed using the same procedure and foundation set in the DMSO phase and compared to experimental results. Later on, at the DFT/B3LYP/6-311++G (d, p) theoretical level, HOMO and LUMO molecular orbital energies, nonlinear optical properties (NLO), and molecular electrostatic potential (MESP) maps will be investigated. The calculated theoretical results will be understood by comparing them to the current experimental values. Gaussian 09(Linux) and Gauss View 5 package programs will be used for all computations.

4. RESULTS AND DISCUSSION

4.1 Geometrical Optimization of the N^2 ,N^6 -bis-[4-(aminosulfonyl) Phenyl]-pyridine-2,6-dicarboxamide) Benzenesulfonamide

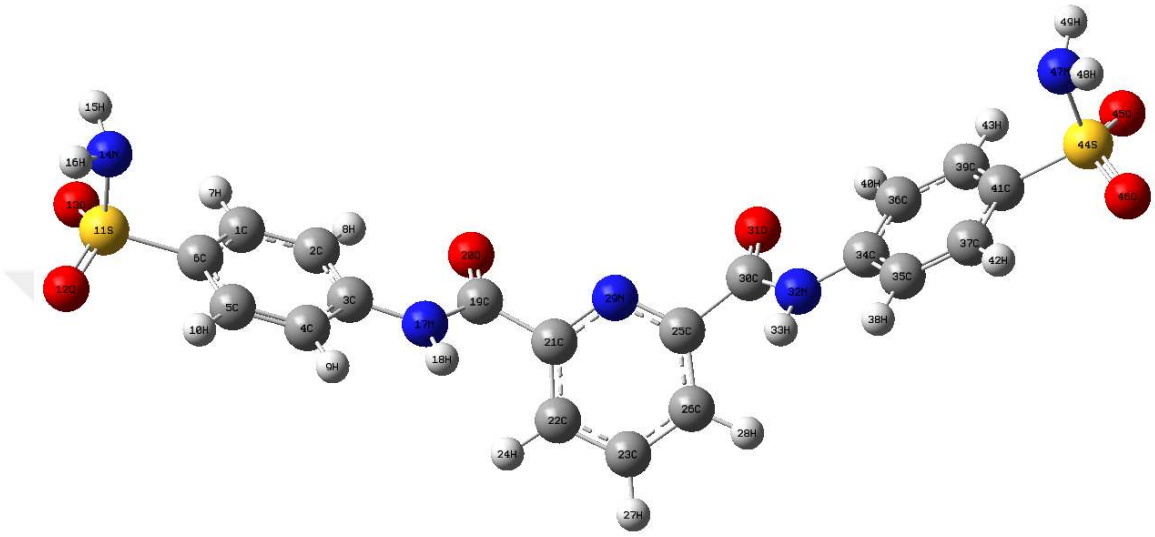

Figure 4. 1 Optimized structures of of N^2 ,N^6 -bis-[4-(aminosulfonyl)phenyl]-pyridine 2,6-dicarboxamide) benzenesulfonamide compound

With the program Gauss View 5.0 and Gaussian 09, the three-dimensional geometry of the molecule was first drawn, and then the entire geometry was drawn. The DFT/B3LYP/6-311++G .(d, p). approach has been used to optimize the molecular system, and the lowest energy structure was discovered (Figure 4.1).

In Table 4.1 shows the bond lengths, bond angles, and Torsion Angle of the compound. According to our current knowledge of the literature, no experimental data on the compound's structural parameters has been uncovered. As a result, key structural properties were compared to those of comparable molecules examined in the literature. the **S-O** bond length was experimentally determined as 1.432 Å and 1.437Å; they found 1.459Å and 1.461Å theoretically by Alyar *et al.* (2012). In this study, the S-O bond length was calculated as 1.461Å.

The S-N bond length was measured to be 1.623Å and theoretically calculated 1.694 by Alyar *et al.* (2012). In this study, it was calculated as 1.695Å. Alyar measured the N-C bond length as 1.470Å experimentally and calculated 1.468Å theoretically. In this study, the N-C bond length was calculated as 1.382Å and 1.407Å. Finally, Alyar measured the C-C bond length as 1.392Å experimentally and calculated 1.402Å theoretically. In this study, the bond C-C length was calculated as 1.402Å**.** These results show us that our theoretical calculations are compatible with the experimental and theoretic data found in the literature for similar molecular systems.

Table 4.1 Molecular geometric parameters (bond lengths, bond and torsion angles) of N^2 ,N^6 -bis-[4-(aminosulfonyl)phenyl]-pyridine-2,6- dicarboxamide) enzenesulfonamide compound

Bond Lenght	**B3LYP6-311++G(d,p).**	**Bond Angles**	**B3LYP6-311++G(d,p).**	**Torsion Angle**	**B3LYP6-311++G(d,p).**
C1-C2	1.391	C2-C1-C6	120.2	C6-C1-C2-C3	0.3
C1-C6	1.391	C2-C1-H7	119.89	C6-C1-C2-H8	-179.7
C1-H7	1.083	C6-C1- H7	119.88	H7-C1-C2-C3	-178.8
C2-C3	1.402	C1-C2-C3	119.46	H7-C1-C2-H8	1.1
C2-H8	1.078	C1-C2-H8	120.63	C2-C1-C6-C5	-0.7
C3-C4	1.404	C3-C2- H8	119.90	C2-C1-C6-S11	179.4
C3-N17	1.407	C2-C3-C4	119.66	H7-C1-C6-C5	178.3
C4-C5	1.385	C2-C3-N17	123.19	H7-C1-C6-S11	-1.4
C4-H9	1.085	C4-C3- N17	117.13	C1-C2-C3-C4	0.2
C5-C6	1.393	C3-C4-H5	120.68	C1-C2-C3 –N17	179.4
C5-H10	1.082	C3-C4-H9	119.85	H8-C2-C3-C4	-179.7
C6-S11	1.792	C5-C4-H9	119.46	H8-C2-C3-N17	-0.5
S11-O12	1.461	C4-C5-C6	119.13	C2-C3-C4-C5	-0.3
S11-O13	1.461	C4-C5-H10	120.64	C2-C3-C4-H9	179.2
S11-N14	1.695	C6-C5-H10	120.21	N17-C3-C4-C5	-179.5
N14-H15	1.015	C1-C6-C5	120.83	N17-C3-C4-H9	0.006
N14-H16	1.015	C1-C6-S11	119.78	C2-C3-N17 –H18	179.5
N17-C19	1.382	C6-S11-O12	107.81	C4-C3-N17 –H18	-1.2
C19-O20	1.211	C6-S11-O13	107.50	C4-C3-N17 –C19	-175.3
C19-C21	1.519	C6-S11-N14	103.67	C3-C4-C5-C6	-0.1
C21-C22	1.399	O12-S11-O13	122.43	C3-C4-C5-H10	178.9
C21-N29	1.333	O12-S11-N14	106.12	H9-C4-C5-C6	-179.6
C22-C23	1.390	O13-S11-N14	107.78	H9-C4-C5-H10	-0.6
C22-H24	1.083	S11-N14-H15	110.51	C4-C5-C6-C1	0.6
C23-C26	1.390	S11-N14-H16	109.70	C4-C5-C6-S11	-179.5
C23-H27	1.083	H15-N14-H16	111.63	H10-C5-C6-C1	-178.4

Table 4.1 (continued)

C25-C26	1.399	C3-N17-H18	115.13	H10-C5-C6-S11	1.4
C25-N29	1.333	C3-N17-C19	128.77	C1-C6-S11-O12	155.6
C25-C30	1.519	H18-N17-C19	115.85	C1-C6-S11-O13	21.8
C26-H28	1.083	N17-C19-O20	124.85	C1-C6-S11-N14	-92.1
C30-O31	1.211	N17-C19-C21	113.26	C5-C6-S11-O12	-24.1
C30-N32	1.382	O20-C19-C21	121.87	C5-C6-S11-O13	-157.9
N32-H33	1.009	C19-C21-C22	121.20	C5-C6-S11-N14	88.05
N32-C34	1.407	C19-C21-N29	115.59	C6-S11-N14-H15	110.7
C34-C35	1.404	C22-C21-N29	123.12	C6-S11-N14-H16	-125.7
C34-C36	1.401	C21-C22-C23	118.40	O12-S11-N14-H15	-135.8
C35-C37	1.385	C21-C22-H24	120.73	O12-S11-N14-H16	-12.3
C35-H38	1.085	C23-C22-H24	120.82	O13-S11-N14-H15	-3.06
C36-C39	1.391	C22-C23-C26	118.80	O13-S11-N14-H16	120.4
C36-H40	1.078	C22-C23-H27	120.59	C3-N17-C19-O20	0.07
C37-C41	1.393	C26-C23-H27	120.59	C3-N17-C19-C21	-178.7
C37-H42	1.082	C26-C25-N29	123.12	H18-N17-C19-O20	-173.9
C39-C41	1.391	C26-C25-C30	121.20	H18-N17-C19-C21	7.1
C39-H43	1.082	N29-C25-C30	115.59	N17-C19-C21-C22	51.7
S44-O45	1.461	C23-C26-H28	120.81	O20-C19-C21-C22	-127.1
S44-O46	1.4617	C25-C26-H28	120.73	O20-C19-C21-N29	49.7
S44-N47	1.695	C21-N29-C25	118.11	C19-C21-C22-C23	176.8
N47-H48	1.015	C25-C30-O31	121.87	C19-C21-C22-H24	-0.9
N47-H49	1.015	C25-C30-N32	113.26	N29-C21-C22-C23	0.1
		O31-C30-N32	124.85	N29-C21-C22-H24	-177.6
		C30-N32-H33	115.85	C19-C21-N29-C25	-178.4
		C30-N32-C34	128.77	C22-C21-N29-C25	-1.5
		H33-N32-C34	115.13	C21-C22-C23 -C26	1.2
		N32-C34-C35	117.13	C21-C22-C23-H27	-178.08
		N32-C34-C36	123.19	H24-C22-C23-C26	179.06
		C35-C34-C36	119.66	H24-C22-C23-H27	-0.3
		C34-C35-C37	120.68	C22-C23-C26-C25	-1.2
		C34-C35-H38	119.85	C22-C23-C26-H28	-179.06
		C37-C35-H38	119.46	H27-C23-C26-C25	178.08
		C34-C36-C39	119.46	H27-C23-C26-H28	0.3
		C34-C36-H40	119.90	N29-C25-C26-C23	-0.1
		C39-C36-H40	120.63	N29-C25-C26-H28	177.6
		C35-C37-C41	119.13	C30-C25-C26-C23	-176.8
		C35-C37-H42	120.64	C30-C25-C26-H28	0.9
		C41-C37-H42	120.21	C26-C25-N29-C21	1.5
		C36-C39-C41	120.21	C30-C25-N29-C21	178.4
		C36-C39-H43	119.89	C26-C25-C30-O31	127.1
		C41-C39-H43	119.88	C26-C25-C30-N32	-51.7
		C37-C41-C39	120.83	N29-C25-C30-O31	-49.7
		C37-C41-S44	119.38	N29-C25-C30-N32	131.3
		C39-C41-N44	119.78	C25-C30-N32-H33	-7.1
		C41-S44-O46	107.81	O31-C30-N32-H33	173.9
		C41-S44-N47	103.67	O31-C30-N32-C34	-0.07
		O45-S44-O46	122.43	C30-N32-C34-C35	175.3
		O45-S44-N47	107.77	C30-N32-C34-C36	-5.4
		O46-S44-N47	106.12	H33-N32-C34-C35	1.2

Table 4.1 (continued)

		S44-N47-H48	109.70	H33-N32-C34-C36	-179.5
		S44-N47-H49	110.51	N32-C34-C35-C37	179.5
		H48-N47-H49	111.63	N32-C34-C35-H38	-0.006
				C36-C34-C35-C37	0.30
				C36-C34-C35-H38	-179.2
				N32-C34-C36-C39	-179.4
				N32-C34-C36-H40	0.54
				C35-C34-C36-C39	-0.2
				C35-C34-C36-H40	179.7
				C34-C35-C37-C41	0.1
				C34-C35-C37-H42	-178.9
				H38-C35-C37-C41	179.6
				H38-C35-C37-H42	0.6
				C34-C36-C39-C41	-0.2
				C34-C36-C39-H43	178.8
				H40-O36-C39-C41	179.7
				H40-O36-C39-H43	-1.1
				C35-C37-C41-C39	-0.6
				C35-C37-C41-S44	179.5
				H42-C37-C41-C39	178.4
				H42-C37-C41-S44	-1.4
				C36-C39-C41-C37	0.7
				H43-C39-C41-C37	-178.3
				H43-C39-C41-S44	1.4
				C37-C41-S44-O45	157.9
				C37-C41-S44-O46	24.1
				C37-C41-S44-N47	-88.06
				C39-C41-S44-O45	-21.8
				C39-C41-S44-O46	-155.6
				C39-C41-S44-N47	92.1
				C41-S44-N47-H48	125.7
				C41-S44-N47-H49	-110.7
				O45-S44-N47-H48	-120.4
				O45-S44-N47-H49	3.02
				O46-S44-N47-H48	12.2
				O46-S44-N47-H49	135.7
				O45-S44-N47-H49	3.02
				O46-S44-N47-H48	12.2
				O46-S44-N47-H49	135.7

4.2 Vibrational Studies

It is not possible to observe all vibrational modes of molecules in experimental spectra. Therefore, theoretical IR calculations play an important role in determining vibration types in molecules. Theoretical IR spectrum values of the molecule were performed on the DFT/B3LYP and 6-311G++(d,p) baseset. N^2 , N^6 -bis-[4-(aminosulfonyl)phenyl]-

pyridine-2,6-dicarboxamide) molecule has 49 atoms and 141 vibrational movements are observed. The N^2 , N^6 -bis-[4-(aminosulfonyl)phenyl]-pyridine-2,6-dicarboxamide) molecule's experimental FT-IR spectrum is shown in Figure 4.2. In this section, experimental and theoretical vibration frequencies are provided (Table 4.2).

We analyzed certain essential characteristic vibrational frequencies of N^2 , N^6 -bis-[4-(aminosulfonyl)phenyl]-pyridine-2,6-dicarboxamide) and compared them to experimental values in order to assign observed peaks. As seen in Table 4.2. the calculated vibrational data agree well with the experimental results.

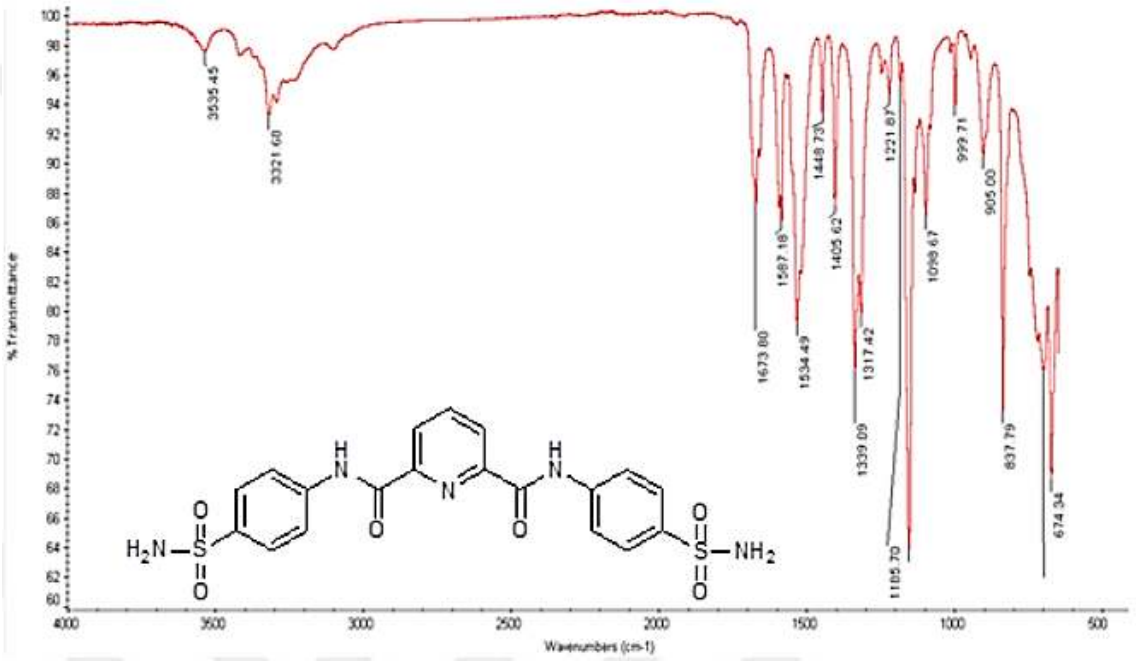

Figure 4.2 FT-IR spectrum of N^2 , N^6 -bis-[4-(aminosulfonyl)phenyl]-pyridine-2,6-dicarboxamide) (Baykan 2019)

N-H_2 stretching vibrations for different molecules were observed between 3500-3300 cm^{-1} (George 2001). Also Baykan observed the NH stretching vibration at 3321 cm^{-1} (Baykan 2019). In this study, we calculated the NH_2 stretching vibration at 3614, 3609 cm^{-1}.And the symmetric stretching vibrations of NH vibrations are calculated at 3508 cm^{-1}. Aromatic compounds have C-H stretching vibrations at about 3000 cm^{-1} (Alyar *et al.*2012). Dikmen measured the C-H stretching vibrations at 3097 cm-1 and 3124 cm^{-1}, and calculated them to be 3065 cm^{-1} (Dikmen 2019). In this study, we calculated the C-H stretching vibrations at 3346, 3205, 3202, 3195, 3185,3174, and 3160 cm^{-1}.

Wojciechowski and Aschaffenburg measure the C-N stretching vibrations at 1238 and 1237 cm^{-1} and calculate their value to be 1235 cm^{-1} (Wojciechowski and Michalska 2007, Aschaffenburg and Moog 2009). In this study, we calculated the C-N stretching vibrations at 1263 and 1261 cm^{-1}. Baykan observed the C=O stretching vibration at 1674 cm^{-1} (Baykan 2019). In this study, the C=O stretching vibration calculated at 1777 and 1773 cm^{-1}.

Aromatic C-C stretching modes of piperazine derivatives were observed between 1650 and 1610 cm^{-1} (Alver *et al.* 2007). In this study, we calculated the aromatic C-C stretching vibrations at 1636, 1635, 1628, 1627, 1616, and 1608 cm^{-1}.

S=O vibrations SO_2 symmetric and asymmetric stretching vibrations occur at 1160 ± 30 cm^{-1} and 1330 ± 30 cm^{-1}, respectively (Gündüzalp *et al.* 2014). Baykan observed the S=O asymmetric and symmetric stretching vibration at 1339 and 1155 cm^{-1} (Baykan 2019). In this study, the S = O asymmetric stretching vibrations are calculated at 1313,1312 cm^{-1}. And the symmetric stretching vibrations of SO_2 vibrations are calculated at 1124,1079 cm^{-1}.

Table 4.2 Theoretical and experimental (FT-IR) vibration frequencies of the N^2 , N^6 – bis-[4-(aminosulfonyl)phenyl]-pyridine- 2,6-dicarboxamide)

Mode	Exp. (Baykan 2019)	Calculated	Intensity	Descriptions
141	3535	3614	78.59	$\upsilon_{as}(N_{47}H_2)$
140		3614	12.80	$\upsilon(N_{14}H_2)$
139	3321	3609	35.88	$\upsilon(N_{17}H) + \upsilon(N_{32}H)$
138		3609	2.05	$\upsilon(N_{17}H) + \upsilon(N_{32}H)$
137		3508	70.60	$\upsilon_s(N_{14}H_2) + \upsilon_s(N_{47}H_2)$
136		3508	31.06	$\upsilon_s(N_{14}H_2) + \upsilon_s(N_{47}H_2)$
135		3246	6.80	$\upsilon_s(CH)_{R1+} \upsilon_s(CH)_{R3}$
134		3246	9.18	$\upsilon_s(CH)_{R1+} \upsilon_s(CH)_{R3}$
133		3205	0.93	$\upsilon_s(CH)_{R1+} \upsilon_s(CH)_{R3}$
132		3205	2.37	$\upsilon_s(CH)_{R1+} \upsilon_s(CH)_{R3}$
131		3202	1.28	$\upsilon_{as}(CH)_{R1}$
130		3202	0.90	$\upsilon_{as}(CH)_{R3}$
129		3195	3.97	$\upsilon_s(CH)_{R2}$
128		3185	7.92	$\upsilon_{as}(CH)_{R2}$
127		3174	2.26	$\upsilon_{as}(CH)_{R2}$
126		3160	11.50	$\upsilon_{as}(CH)_{R1+} \upsilon_{as}(CH)_{R3}$
125		3160	12.35	$\upsilon_{as}(CH)_{R1+} \upsilon_{as}(CH)_{R3}$

Table 4.2 (continued)

124	1674	1773	383.85	$\upsilon(C{=}O)_{ring} + \beta(C_{19}NH) + \beta(C_{30}NH)$
123		1777	12.11	$\upsilon(C{=}O)_{ring} + \beta(C_{19}NH) + \beta(C_{30}NH)$
122		1636	17.87	$\upsilon(CC)_{R1,3} + \beta(CCH)_{R1,3}$
121		1635	114.62	$\upsilon(CC)_{R1,3} + \beta(CCH)_{R1,3}$
120		1628	62.49	$\upsilon(CC)_{R1,3} + \beta(C_3NH) + \beta(C_{34}NH)$
119		1627	131.8	$\upsilon(CC)_{R1,3} + \beta(C_3NH) + \beta(C_{34}NH)$
118		1616	37.75	$\upsilon(CC)_{R2} + \upsilon(CN)_{R2} + \beta(CCH)_{R2}$
117		1608	34.01	$\upsilon(CC)_{R2} + \upsilon(CN)_{R2} + \beta(CCH)_{R2}$
116		1586	54.48	$\beta(N_{14}H_2) + \beta(N_{47}H_2)$
115		1586	3.35	$\beta(N_{14}H_2) + \beta(N_{47}H_2)$
114		1547	161.19	$\upsilon(CC)_{R1,3} + \beta(C_3NH) + \beta(C_{30}NH)$
113		1540	104.7	$\upsilon(CC)_{R1,3} + \beta(C_3NH) + \beta(C_{30}NH)$
112		1523	4.04	$\upsilon(CC)_{R1,3} + \beta(C_3NH) + \beta(C_{30}NH)$
111		1523	10.88	$\upsilon(CC)_{R1,3} + \beta(C_3NH) + \beta(C_{30}NH)$
110		1470	19.34	$\upsilon(CC)_{R2} + \upsilon(CN)_{R2} + \beta(CCH)_{R2}$
109		1447	5.83	$\upsilon(CC)_{R2} + \upsilon(CN)_{R2} + \beta(CCH)_{R2}$
108		1426	161.47	$\upsilon(CC)_{R1,2} + \beta(CCH)_{R1,3}$
107		1426	75.48	$\upsilon(CC)_{R1,2} + \beta(CCH)_{R1,3}$
106		1347	99.21	$\upsilon(CC)_{R1,3} + \upsilon(C_3N) + \beta(C_{34}N)$
105		1344	288.50	$\upsilon(CC)_{R1,3} + \upsilon(C_3N) + \beta(C_{34}N)$
104		1329	10.77	$\beta(CCH)_{R1,3}$
103		1329	18.21	$\beta(CCH)_{R1,3}$
102	1339	1313	327.27	$\upsilon_{as}(SO_2)$
101		1312	21.56	$\upsilon_{as}(SO_2)$
100		1294	5.99	$\upsilon(CC)_{R2} + \upsilon(CN)_{R2}$
99		1281	8.16	$\upsilon(C_{19}C) + \upsilon(C_{30}C) + \beta(C_{21}NC)$
98		1263	34.56	$\upsilon(C_3N) + \upsilon(C_{34}N) + \upsilon(CC)_{R1,3}$
97		1261	173.53	$\upsilon(C_3N) + \upsilon(C_{34}N) + \upsilon(CC)_{R1,3}$
96		1236	110.89	$\upsilon(C_{30}C) + \upsilon(C_{19}C) + \beta(CCH)_{R2}$
95		1206	5.90	$\beta(CCH)_{R1,3}$
94		1206	12.86	$\beta(CCH)_{R1,3}$
93		1188	85.35	$\upsilon(CC)_{R2} + \beta(CCH)_{R2}$
92		1159	163.01	$\upsilon(CC)_{R2} + \upsilon(C_{19}N) + \upsilon(C_{30}N) + \beta(CCH)_{R2}$
91		1147	36.28	$\beta(CCH)_{R1,3}$
90		1142	6.75	$\beta(CCH)_{R1,3}$
89		1132	29.90	$\upsilon(CC)_{R1,3} + \upsilon(N_{17}C) + \upsilon(N_{32}C) + \beta(CCH)_{R1,3}$
88		1125	399.85	$\upsilon(CC)_{R1,3} + \upsilon(N_{17}C) + \upsilon(N_{32}C) + \beta(CCH)_{R1,3}$
87	1155	1124	7.77	$\upsilon(CC)_{R1,2,2} + \upsilon(C_6S) + \upsilon(C_{41}S) + \upsilon_s(S_{44}{=}O) + \upsilon_s(S_{11}{=}O)_{R1,3}$
86		1110	5.08	$\upsilon(CC)_{R2} + \beta(CCH)_{R2}$
85		1091	0.94	$\rho(N_{14}H_2) + \rho(N_{47}H_2)$
84		1091	10.82	$\rho(N_{14}H_2) + \rho(N_{47}H_2)$
83		1079	106.13	$\upsilon(C_{41}S) + \upsilon(C_6S) + \upsilon_s(S_{11}{=}O) + \upsilon_s(S_{44}{=}O)$
82		1079	57.72	$\upsilon(C_{41}S) + \upsilon(C_6S) + \upsilon_s(S_{11}{=}O) + \upsilon_s(S_{44}{=}O)$
81		1026	5.68	$\upsilon(CC)_{R1,3} + \beta(CC)_{R1,3}$
80		1026	4.51	$\upsilon(CC)_{R1,3} + \beta(CC)_{R1,3}$
79		1015	0.16	$\gamma(CC)_{R2}$
78		1007	5.10	$\beta(CCC)_{R2} + \beta(CNC)_{R2}$
77		1000	1.25	$\gamma(CH)_{R1,3}$
76		1000	0.13	$\gamma(CH)_{R1,3}$
75		964	0.23	$\gamma(CH)_{R1,3}$
74		964	0.04	$\gamma(CH)_{R1,3}$

Table 4. 2 (Continued)

73		950	9.33	$\upsilon(C_{30}C) + \gamma(C_{19}C) + \beta(N_{17}C=O) + \beta(N_{32}C=O)$
72		938	1.69	$\gamma(CH)_{R2}$
71		898	18.84	$\beta(N17\,C=O) + \beta(N_{32}\,C=O)$
70		868	6.01	$\gamma(CH)_{R1,3}$
69		867	20.99	$\gamma(CH)_{R1,3}$
68		866	120.3	$\upsilon(SN) + \gamma(CH)_{R1,3}$
67		862	36.47	$\tau(NCCH) + \tau(NCCC) + \tau(CCCC) + \tau(CCCH)$
66		849	128.6	$\upsilon(SN) + \beta(S\text{-}NH_2) + \tau(CH)_{R1,2,3}$
65		844	224.5	$\upsilon(SN) + \beta(S\text{-}NH_2)$
64		828	40.0	$\tau(CH)_{R1,3}$
63		828	0.49	$\tau(CH)_{R1,3}$
62		817	27.17	$\beta(CCC)_{R1,3} + \tau(CH)_{R2}$
61		791	21.96	$\tau(N_{29}CCO) + \tau(N_{29}CCN)$
60		768	22.37	$\tau(CH)_{R2} + \tau(NCCH)_{R2} + \tau(NCCC)_{R2}$
59		731	38.85	$\beta(CCC)_{R1,2,3}$
58		734	2.13	$\tau(CCCC)_{R1.3} + \tau(CCCH)$
57		732	5.76	$\tau(CCCC)_{R1.3} + \tau(CCCH)_{R1.3}$
56		726	1.75	$\tau(CCCC)_{R1.3} + \tau(CCCH)_{R1.3} + \tau(C_{24}NCO) + \tau(C_{24}NCC)$
55		695	48.44	$\upsilon(SN) + \beta(CCC)_{R1,2,3} + \beta(C_{25}CN)$
54		679	17.45	$\upsilon(SN) + \beta(CCC)_{R1,2,3} + \beta(C_{25}CN)$
53		648	5.55	$\beta(CCC)_{R1,2,3} + \beta(CNC)_{R2}$
52		642	0.49	$\beta(CCC)_{R1,2,3} + \beta(CNC)_{R2}$
51		639	24.75	$\upsilon(SN) + \beta(CCC)_{R1,2,3} + \beta(S\text{-}NH_2)$
50		637	90.89	$\beta(S\text{-}NH_2)$
49		636	382.97	$\beta(S\text{-}NH_2)$
48		603	115.09	$\beta(S\text{-}NH_2) + \tau(CCCN) + \tau(NCCH)$
47		569	19.39	$\gamma(N_{17}H) + \gamma(N_{32}H)$
46		569	55.09	$\gamma(N_{17}H) + \gamma(N_{32}H)$
45		554	146.98	$\beta(N\text{-}SO_2) + \tau(CCCH)_{R1,3} + \tau(CCCC)_{R1,3}$
44		550	0.65	$\tau(CCCC)_{R1,3} + \tau(CCCH)_{R1,3}$
43		540	9.11	$\tau(CCCC)_{R1,3} + \tau(CCCH)_{R1,3}$
42		532	67.83	$\beta(N\text{-}SO_2) + \tau(CCCH)_{R1,3} + \tau(CCCC)_{R1,3}$
41		484	6.27	$\tau(NCCC)_{R2} + \tau(NCCH) + \tau(CCCC)_{R2}$

υ_s: symmetric stretching, υ_{as}: asymmetric stretching, β: in-plane bending, γ: out-of-plane bending, τ: torsion, umb: umbrella.

4.3 NMR Spectra

^{1}H-NMR spectra of N^2 , N^6 -bis-[4-(aminosulfonyl)phenyl]-pyridine- 2,6-dicarboxamide) were measured and interpreted in DMSO by Baykan (Baykan 2019). In order to facilitate the interpretation of NMR spectra, quantum-chemical calculations were performed using B3LYP/6-311++G(d,p) basis set in DMSO phase. Only ^{1}H-NMR values of N^2 , N^6 -bis-[4-(aminosulfonyl)phenyl]-pyridine- 2,6-dicarboxamide) have

been found in the literature. The obtained values in the study are given in Table 4.3 together with the experimental values. The ^{1}H-NMR spectrum of N^{2} , N^{6} -bis-[4-(aminosulfonyl)phenyl]-pyridine- 2,6-dicarboxamide) presented in Figure 4.3. When the ^{1}H-NMR spectrum of 128 compounds is examined; At δ 7.36 ppm, singlet belonging to sulfonyl-linked NH_2 protons and a total of 8 aromatic protons in the range of δ 7.91-8.15 ppm resonated as two doublet signals. δ Between 8.36-8.46 ppm, peak groups of 3 protons attached to the pyridine ring were observed. δ At 11.29 ppm, the characteristic N-H proton signal of carboxyamide was observed.

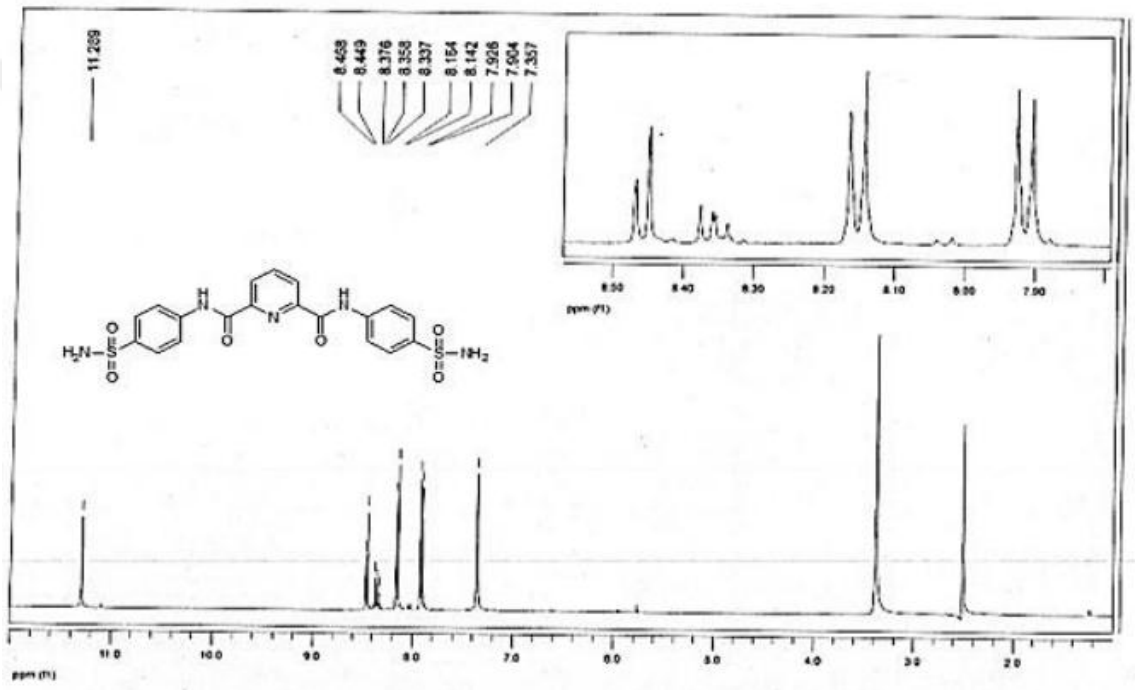

Figure 4.3 ^{1}H-NMR spectrum of N^{2} , N^{6} -bis-[4-(aminosulfonyl)phenyl]-pyridine-2,6-dicarboxamide) (Baykan 2019)

Table 4.3 The experimental and theoretical ^{1}H and ^{13}C NMR chemical shifts δ(ppm) for N^{2},N^{6}-bis-[4-(aminosulfonyl)phenyl]-pyridine-2,6-dicarboxamide)

Assignment	B3LYP/6-311++G(d,p) $\delta exp.$ (Baykan 2019)	B3LYP/6-311++G(d,p)[a] δcalculated
^{1}C		127.84
^{2}C		117.47
^{3}C		144.06
^{4}C		118.60
^{5}C		126.48
^{6}C		141.63
^{19}C		164.89

Table 4. 3 (continued)

^{30}C		164.89
^{21}C		155.88
^{25}C		155.88
^{34}C		144.06
^{41}C		141.63
^{23}C		140.06
^{39}C		127.84
^{37}C		126.48
^{22}C		126.48
^{26}C		123.64
^{35}C		118.60
^{36}C		117.47
^{40}H	8.15	8.98
^{8}H	8.15	9.98
^{27}H	8.46	8.15
^{43}H	7.91	7.88
^{7}H	7.91	7.88
^{24}H	8.36	7.76
^{28}H	8.36	7.76
^{33}H	7.91	7.61
^{18}H	7.91	7.61
^{10}H	7.91	7.60
^{42}H	7.91	7.60
^{9}H	7.36	7.09
^{38}H	7.36	7.09
^{16}H	7.36	4.14
^{48}H	7.36	4.14
^{49}H	7.36	4.00
^{15}H	7.36	4.00

σ Transform into using equations given in Refs (Blanco *et al.* 2007, Silva *et al.* 2008) $\sigma^{13}\mathrm{C} = 175.7 - 0.963\ \sigma^{13}\mathrm{C}$ and $\sigma^{1}\mathrm{H} = 31.0 - 0.970\ \sigma^{1}\mathrm{H}$.

4.4 HOMO-LUMO Analyze

Molecule boundary orbitals are commonly used to describe chemical interactions between molecules. The boundary orbitals in this context refer to the highest occupied orbital (HOMO) and the lowest-energy empty molecular orbital (LUMO). Because most chemical changes involve the acquisition or loss of electrons, HOMO & LUMO have a direct impact on the chemical behavior of the molecules. The lower the energy of the lowest energy empty molecular orbital (LUMO), in which the electron to be taken will be put, the easier it will be to take the electron. Because electrons will be donated from the maximum energy filled molecule orbital (HOMO), the higher the energy of this orbital, the greater the proclivity to donate electrons. The three-dimensional HOMO-

LUMO graph of the complex N^2 ,N^6 -bıs-[4-(amınosulfonyl)phenyl]-pyrıdıne-2,6-dıcarboxamıde are shown in Figure 4.4 The HOMO and LUMO energy values of the compounds were calculated on the 6-311++G.(d,p). basis set of the B3LYP method. According to the calculation, the energy band gap between the ground state and first excited levels of the compounds are around 4.685 eV. The highest molecular orbital that is occupied energy indicates an electron's capacity to give, while the lowest unoccupied molecular orbital energy indicates an electron's ability to recognize, and the energy gap reflects the molecules' chemical reactivity and kinetic stability. As can be observed in Figure 4.4 the HOMO orbital is placed over nitrogen and carbon atoms; the transition from the HOMO orbital to the LUMO orbital represents an electron density transfer from nitrogen to carbon atoms in the ring. Figure 4.4 depicts the HOMO LUMO energy gap of N^2 ,N^6 -bıs-[4-(amınosulfonyl)phenyl]-pyrıdıne-2,6-dıcarboxamıde guanidine calculated using the DFT/B3LYP technique at the 6-311++G(d, p) level, indicating that the energy gap represents the molecule's chemical activity. The small energy difference between HOMO and LUMO energies allows for economical intramolecular charge transfer. It activates the substance NLO (Kanmazalp 2017).

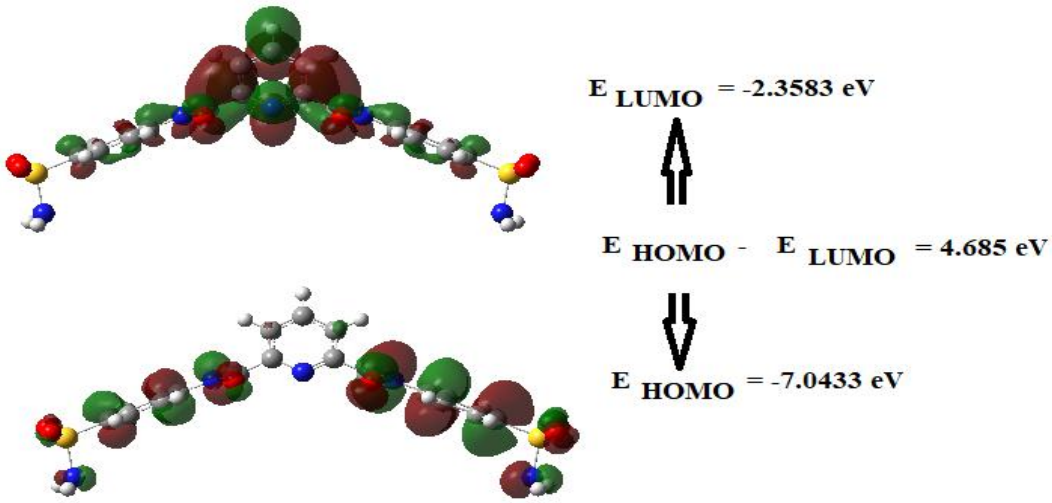

Figure 4.4 Energy levels and the 3D plots of the HOMO and LUMO of the N^2,N^6-bis-[4-(aminosulfonyl)phenyl]-pyridine-2,6-dicarboxamide compound at the B3LYP/6−311++G(d,p) level.

4.5 Nonlinear Optical (NLO) Properties

NLO materials have piqued the interest of researchers in past few years because of their prospective uses in optoelectronics, namely telecommunications, optical computing, optical data storage, optical switching, and different photonic technologies (Prasad and Williams 1991). Polarizability determines optical characteristics of organic materials. An atom's or molecule's polarizability is a measure of how easily the nucleus and electrons may be shifted from their stable states. The valence electrons farthest from the nucleus are the most easily moved in an atom or molecule. As a result, it makes a significant contribution to the polarizability of valence electrons. The dipole moment (μ), static polarizability (α_0), and initial static hyperpolarizability (βtot) are all strongly connected to NLO activity.

The polarizabilities and hyperpolarizabilities derived from Gaussian 09 output were translated from atomic units to electrostatic units (α: 1a.u = $0.1482*10^{-24}$esu; β: 1a.u = $8.6393*10^{-33}$esu) (Sundaraganesan *et al.* 2009). Total static dipole moment, μ is defined as; $\mu = (\mu_x^2 + \mu_y^2 + \mu_z^2)^{1/2}$. The computations of static polarizability (α_{ave}) and initial static hyperpolarizability (β_{tot}) from the Gaussian output are detailed below (Alyar *et al.* 2007):

$$\langle\alpha\rangle = 1/3\ (\alpha_{xx} + \alpha_{yy} + \alpha_{zz}\ )$$

$$\beta_{tot} = [(\beta_{xxx} + \beta_{xyy} + \beta_{xzz})^2 + (\beta_{yyy} + \beta_{yzz} + \beta_{yxx})^2 + (\beta_{zzz} + \beta_{zxx} + \beta_{zyy})^2]^{1/2}$$

Because of its characteristics in the research of nonlinear optical properties, urea is regarded a generic reference. The NLO characteristics of the molecules under consideration are assessed by comparing them to urea. Calculations with DFT/B3LYP/6-311G(d) yielded urea values of μ = 1.3732 Debye, α = 3.8312 $Å^3$ and $\beta = 0.37289.10^{-30}$ cm^5/esu . Theoretical calculations on molecule hyperpolarizability (β) are extremely valuable in understanding the link between molecular structure and nonlinear optical characteristics. However, determining hyperpolarizability is a tough

process. An alternative option is a direct computational calculation (Kleinmann 1962). Urea is one of the archetypal molecules. utilized in the investigation of molecular nonlinear characteristics systems (Kanmazalp 2017). As a result, it is commonly employed as a threshold. value for comparative purposes. The first hyperpolarizable (β_0) of this molecular system and associated characteristics (α total and $\Delta\alpha$) are estimated at the B3LYP/6-311+G(d,p) level, their and Table 4.4 displays the computed values.

Table 4.4 The electric dipole moment μ (D), t he mean polarizability <α> and the first hyperpolarizability (βtot) of N^2,N^6-bis-[4-(aminosulfonyl)phenyl]-pyridine-2,6-dicarboxamide by DFT/B3LYP/6- 311++G(d,p) level of theory.

Parameter	**N^2,N^6-bis-[4-(aminosulfonyl)phenyl]-pyridine-2,6-dicarboxamide**	**Parameter**	**N^2,N^6-bis-[4-(aminosulfonyl)phenyl]-pyridine-2,6-dicarboxamide**
μ_x	0.0002	β_{xxx}	-0.38
μ_y	0.0478	β_{xxy}	193.58
μ_z	-3.0011	β_{xyy}	0.81
μ_{tot}	3.0014	β_{yyy}	26.62
α_{xx}	505.51	β_{xxz}	271.98
α_{xy}	-0.00	β_{xyz}	0.06
α_{yy}	257.44	β_{yyz}	3.49
α_{xz}	-0.00	β_{xzz}	-0.08
α_{yz}	-17.02	β_{yzz}	56.14
α_{zz}	276.32	β_{zzz}	-138.29
<α> (a.u)	346.42	**β_{tot} (a.u)**	308.5
<α> (esu)	51.34 x 10^{-24} esu	**β_{tot} (esu)**	2665.2 x10^{-33} esu

α: 1a. u = 0.1482*10^{-24} esu, β: 1a. u = 8.6393*10^{-33}esu

The (μ) dipole moment and mean polarizability (α tot) were determined to be 3.0014 D and 51.34 x 10^{-24} esu, respectively. Furthermore, the compound's 1st order hyperpolarizability was determined to be 2665.2 x10^{-33} esu. Based on the finding, we conclude that the title chemical and its derivatives are a promising target for future nonlinear optical property research.

4.6 Molecular Electrostatic Potential (MESP)

The MEP surface usually provides information about the chemical reactivity of any molecule. used to acquire. MEP is electrostatic between proton and molecule relates to interaction (Abragam 1961).

MESP maps are concerned with a molecule's electronic density. This is an excellent descriptor for understanding hydrogen bond interactions and locating hydrogen bond locations in electrophilic and nucleophilic processes (Yeşilkaynak *et al*. 2010).

It provides information based on color changes. MEP is a molecular Bridge for some information such as molecule size and shape that must be learnt for functions. (Mlynarek 1986, Weiss *et al.* 2012).

The molecular electrostatic potential energy of N^2,N^6-bis-[4-(aminosulfonyl)phenyl]-pyridine-2,6-dicarboxamide surfaces. Figure 4.5 shows compound created using the DFT/B3LYP/6-311++G .(d, p). model. When looking at the colors of the compounds on this map, it is clear that the red areas have an excess of electrons, indicating that they are negatively charged. The blue patches are positively charged because it seems as though there aren't enough electrons in them. When an electron is reduced, the surrounding area gradually turns blue, while when an electron is received, the surrounding area gradually turns red. Positive (blue) areas are related to nucleophilic reactivity, whereas negative (red) regions are related to electrophilic reactivity. The electron distribution for each component is clearly displayed on the MESP map. Their blue and red shifts may be examined by examining the locations of the nitrogen and oxygen atoms on the molecules. These findings offer crucial data on the region's bond structure and intermolecular interactions.

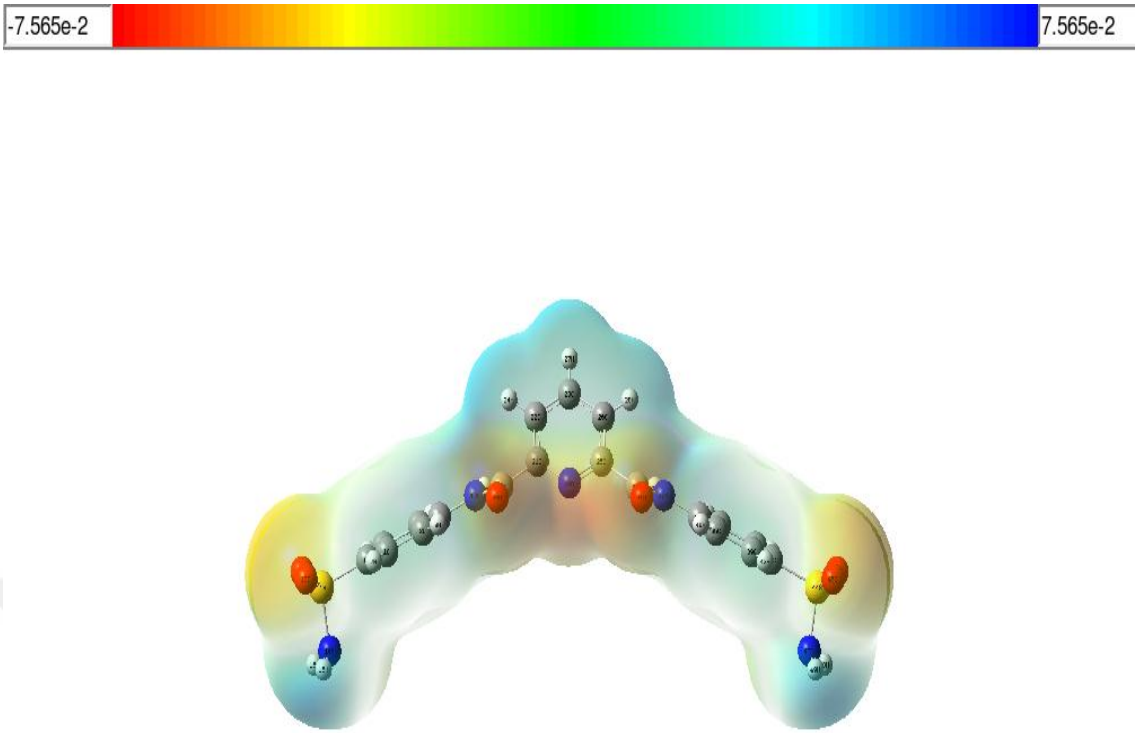

Figure 4.5 MESP map of N^2,N^6-bis-[4-(aminosulfonyl)phenyl]-pyridine-2,6-dicarboxamide

5. CONCLUSION AND RECOMMENDATION

In the study, N^2,N^6-bis-[4- (aminosulfonyl) phenyl] -pyridine-2,6-dicarboxamide molecule was experimentally synthesized by Adem Rıza Baykan. First of all, the stable structure with minimum energy of the studied molecule was obtained by DFT method by performing geometry optimization calculation at B3LYP/6-311++G(d,p) level. Since the molecule studied in the literature has no experimental structural parameters, the theoretically calculated bond lengths and bond angles of the compound were compared with the experimental values of similar molecules in the literature. The S-O, S-N and N-C bond lengths were calculated as 1.461, 1.695 and 1.382 Å. It was seen that the calculated results and the experimental values in the literature were compatible with each other. In the FT-IR analysis results obtained with the 6-311++G(d,p) basis set we used with the DFT/B3LYP method, it is seen that the values of 1263 and 1261 cm^{-1} calculated for the C-N stretching vibration coincide with the values of similar molecule groups in the literature (Kozhevina *et al.* 1995). In addition, the absence of virtual vibration frequency values (negative number) indicates that the molecule is optimized with correct calculation methods and has a stable structure. After examining the vibration frequencies of the studied molecule, ^{1}H-NMR and ^{13}C-NMR chemical shift values were calculated. The HOMO and LUMO energies of the N^2,N^6-bis-[4-(aminosulfonyl)phenyl]-pyridine-2,6-dicarboxamide molecule were calculated by the DFT method at the B3LYP/6-311++G(d,p) level. The obtained HOMO and LUMO energy difference was found to be 4.685 eV. The nonlinear optical properties and molecular potential energy surface map of the studied compound were calculated using the same method and basis set. As a result of calculation, the compound was found to have a hyperpolarizability of 2665.2 $x10^{-33}$ esu. This value indicates that the hyperpolarizability of the compound is approximately 7.15 times greater than that of urea. Therefore, it can be said that the compound exhibits nonlinear optical properties. On the molecular potential energy surface, the red regions indicate electron-rich regions, and the gray and blue regions indicate electron-poor regions. In this thesis, all calculations were performed with Gaussian 09 (Linux) and Gauss View 5.0 package program.

REFERENCES

Abragam, A. 1961. The principles of nuclear magnetism (No. 32). Oxford university press, 599 page, USA.

Adkins, J. C. and Faulds, D. 1998. Amprenavir. Drugs, 55(6): 837-842.

Agarwal, B. K. 2013. X-ray spectroscopy: an introduction (Vol. 15). Springer, 421 page, USA.

Al-Sammarraie, M.j. 2021. illumination of the structures of some sulfonamide compounds with biological activity by spectroscopic physical properties by methods and investigation of their dft method . MSc. Thesis, Çankiri karatekin university, 72 page, Çankiri.

Altgelt, C. A. 2005. The world's largest 'radio'station. Nukewatch, 715: 472-4185.

Alver, Ö., Parlak, C. and Şenyel, M. 2007. FT-IR and NMR investigation of 1-phenylpiperazine: A combined experimental and theoretical study. Spectrochimica Acta Part A: Molecular and Biomolecular Spectroscopy, 67(3-4): 793-801.

Alyar, H., Alyar, S., Unal, A., Ozbek, N., Sahin, E., Karacan, N. 2012. Synthesis, characterization and antimicrobial activity of m-toluenesulfonamide,N,N'-1,2-ethanediylbis (mtsen) and [Cu(II)(phenanthroline)2]mtsen complex. J. Mol. Structure, 1028: 116–125.

Alyar, H., Kantarci, Z., Bahat, M. and Kasap, E. R. G. Ü. N. 2007. Investigation of torsional barriers and nonlinear optical (NLO) properties of phenyltriazines. Journal of molecular structure, 834: 516-520.

Alyar, H., Ünal, A., Özbek, N., Alyar, S. and Karacan, N. 2012. Conformational analysis, vibrational and NMR spectroscopic study of the methanesulfonamide-N, N′-1, 2-ethanediylbis. Spectrochimica Acta Part A: Molecular and Biomolecular Spectroscopy, 91: 39-47.

Aschaffenburg, D. J. and Moog, R. S. 2009. Probing hydrogen bonding environments: solvatochromic effects on the CN vibration of benzonitrile. The Journal of Physical Chemistry B, 113(38): 12736-12743.

Aslan, H. G. 2017. Synthesis, structural characterization and DTA/TG studies of a Schiff base. Süleyman Demirel Üniversitesi Fen Bilimleri Enstitüsü Dergisi, 21(3), 812-815

ATASI, 2019. ATA Scientific Instruments. website: https://www.atascientific.com.au /spectrometry/. Date of access: 20.03.2022.

Atkins, P.W. and de Paula, J. 2009. Elements of physical chemistry (5th ed.). Oxford U.P, 459 page, USA.

Babaoglu, K., Qi, J., Lee, R. E. and White, S. W. 2004. Crystal structure of 7, 8-dihydropteroate synthase from Bacillus anthracis: mechanism and novel inhibitor design. Structure, 12(9): 1705-1717.

Banwell, C. N. and McCash, E. M. 1994. Fundamentals of Molecular Spectroscopy (4th ed.). McGraw Hill, 292 page, UK.

Baykan, A.R. 2019. Synthesıs of Dicarboxysulfonamide Compounds And Their Carbonic Anhydrase (hCA I And hCA II) Enzyme Actıvıty. MSc. Thesis. Ağri İbrahim Çeçen University, 108 Page, Ağrı.

Blanco, F., Alkorta, I. and Elguero, J. 2007. Statistical analysis of 13C and 15N NMR chemical shifts from GIAO/B3LYP/6- 311++ G** calculated absolute shieldings. Magnetic Resonance in Chemistry, 45(9): 797-800.

Born, M. and Oppenheimer, R. 1927. Zur Quantentheorie der Molekeln. Annalen der Physik, 389: 457-484.

Boys, S. F. 1950. Electronic wave functions-I. A general method of calculation for the stationary states of any molecular system. Proceedings of the Royal Society of London. Series A. Mathematical and Physical Sciences, 200(1063): 542-554.

Bradt, H. 2004. Astronomy methods: A physical approach to astronomical observations. Cambridge University Press, 421 page, USA.

Brock, G. 2000. Sildenafil citrate (Viagra®). Drugs Today, 36(2-3): 125.

Bunker, P. R. and Jensen, P. 2006. Molecular symmetry and spectroscopy (Vol. 46853). NRC research press, 752 page, USA.

Chilton, A. 2014. The Working Principle and Key Applications of Infrared Sensors. Infrared Radiation Theory.

Cohen, A. J., Mori-Sánchez, P. and Yang, W. 2012. Challenges for density functional theory. Chemical reviews, 112(1): 289-320.

Colthup, N.B. 1990. Introduction to Kızıl ötesi and raman spectroscopy. Academic Press, 356 page, USA.

Cormen, T. H. 2009. CE Leiserson, RL Rivest, and C. Stein. Introduction to algorithms. The MIT Press, 1313 page, England.

Derome, A.E. 1987. Modern NMR Techniques for Chemistry Research. Oxford Pergamon Press, 280 page, USA.

DİKMEN, G. 2019. 1-(4-chlorophenyl) Piperazine: FT-IR, Raman, NMR and Theoretical Studies. Anadolu University Journal of Science and Technology A-Applied Sciences and Engineering, 20(2): 133-142.

Dirac, P. A. M. 1926. "On the Theory of Quantum Mechanics". Proceedings of the Royal Society A. 112 (762): 661–677.

Donald, L. P., George S. Kreese, G. and Lampman, M. 1979. Introduction to spectroscopy. Cengage learning., 215 page, USA..

Dorsett, H. E. and White, A. 2000. Overview of molecular modelling and ab-initio molecular orbital methods suitable for use with energetic materials. DSTO technical report, 46 page, Australia.

Ellingson, S. W. 2016. Radio Systems Engineering. Cambridge University Press, 651 pages, USA.

EMS, 2004. ElectroMagneticspectrum. https://electromagneticspectrumscience.weebly.com/visible-light.html. Date of access: 11.02.2022.

Energy Minimization, 2021. November 23. website: https://en.wikipedia.org/wiki/Energy_minimization . Date of access: 19.02.2022.

Esbaugh, A. J. and Tufts, B. L. 2006. The structure and function of carbonic anhydrase isozymes in the respiratory system of vertebrates. Respiratory physiology & neurobiology, 154(1-2): 185-198.

Extended Basis Sets, 2014. June 17. website: https://chem.libretexts.org/Bookshelves/Physical_and_Theoretical_Chemistry_Textbook_Maps/Physical_Chemistry_(LibreTexts)/11%3A_Computational_Quantum_Chemistry/11.03%3A_Extended_Basis_Sets#mjx-eqn-11.2.1. Date of access: 23.04.2022.

Filler, A. 2009. The history, development and impact of computed imaging in neurological diagnosis and neurosurgery: CT, MRI, and DTI. Nature precedings, 2: 1-1.

Fleming, J. R. 2008. Climate Change and Anthropogenic Greenhouse-Warming: A Selection of Key Articles, 1824–1995, with Interpretative Essays. NSDL Classic Articles in Context, 1: 3-13.

Foresman, J.B. and Frisch, A. 1996. Exploring chemistry with electronic structure Methods. Gaussian Inc., 263 page, USA.

Gandhimathi, R., Vijayaraj, S. and Jyothirmaie, M. P. 2012. Analytical process of drugs by ultraviolet (UV) spectroscopy–a review. International Journal of Pharmaceutical Research & Analysis, 2(2): 72-78.

George, S. 2001. Infrared and Raman characteristic group frequencies: tables and charts. Wiley, 223 page, Chichester.

Gill, P. M. and von Rague Schleyer, P. 1994. Density Functional Theory (DFT), Hartree-Fock (HF), and the self-consistent field. J. Chem. Phys, 100: 5066-5075.

Graves, P. R. G. D. J. and Gardiner, D. 1989. Practical raman spectroscopy. Springer, 10: 978-983.

Greenfield, R. A. and Bronze, M. S. 2003. Prevention and treatment of bacterial diseases caused by bacterial bioterrorism threat agents. Drug discovery today, 8(19): 881-888.

Griffiths, D. J. 1995. Introduction to Quantum Mechanics. Upper Saddle River, New Jersey Prentice Hall, 409 page, USA.

Griffiths, David J. 2004. Introduction to Quantum Mechanics (2nd ed.). Prentice Hall, 326 page, USA.

Gündüzalp, A. B., Özmen, Ü. Ö., Çevrimli, B. S., Mamaş, S. and Cete, S. 2014. Synthesis,characterization, electrochemical behavior, and antimicrobial activities of aromatic/heteroaromatic sulfonylhydrazone derivatives. Medicinal Chemistry Research, 23(7): 3255-3268.

Haigh, J. D. 2007. The Sun and the Earth's climate. Living reviews in solar physics, 4(1): 1-64.

Hall, G. G. 1951. The molecular orbital theory of chemical valency VIII. A method of calculating ionization potentials. Proceedings of the Royal Society of London. Series A. Mathematical and Physical Sciences, 205(1083): 541-552.

Harman, P. M. 1998. The natural philosophy of James Clerk Maxwell. Cambridge University Press, 321 page, UK.

Hartree, D. R. and Black, M. M. 1933. A theoretical investigation of the oxygen atom in various states of ionisation. Proceedings of the Royal Society of London. Series A, Containing Papers of a Mathematical and Physical Character, 139(838): 311-335.

Heisenberg, W. 1926. Mehrkörperproblem und Resonanz in der Quantenmechanik. Zeitschrift für Physik. 38 (6–7): 411–426.

Hitchcock, R. T. 2004. Radio-frequency and Microwave Radiation. American Industrial Hygiene Assn., 2: 332-339.

Hollas, J. M. 1996. Modern Spectroscopy (3rd ed.). John Wiley, 77 page, New York.

Hungund, G. M. 2020. Computational Astronomy: Classification of Celestial Spectra Using Machine Learning Techniques of Physics F: Metal Physics, 4(8): 1170.

Jensen, F. 2017. Introduction to computational chemistry. John Wiley and Sons, 664 page, USA.

Jones, G. A., Layer, D. H. and Osenkowsky, T. G. 2013. National association of broadcasters engineering handbook: NAB engineering handbook. Taylor and Francis, 2120 page, USA.

Kalbasi, R. J. and Mosaddegh, N. 2012. Palladium nanoparticles supported on poly (2-hydroxyethyl methacrylate)/KIT-6 composite as an efficient and reusable catalyst for Suzuki–Miyaura reaction in water. Journal of Inorganic and Organometallic Polymers and Materials, 22(2): 404-414.

Kanmazalp, S. 2017. Karaelmas Fen ve Müh. Web sitesi. https://dergipark.org.tr/en/download/article-file/1329456. Derg, 7(2): 491–496.

Kleinmann, DA. 1962. Nonlinear dielectric polarization in optical media. Phys. Rev., 126: 2-11.

Koirtyohann, S. R. 1991. A history of atomic absorption spectroscopy from an academic perspective. Analytical Chemistry, 63(21): 1024-1031.

Kolaczek, A., Fusiarz, I., Ławecka, J. and Branowska, D. 2014. Biological activity and synthesis of sulfonamide derivatives: a brief review. Chemik, 68(7): 620-628.

Kozhevina, L. I., Prokopenko, E. B., Rybachenko, V. I. and Titov, E. V. 1995. The influence of the fluorosubstituence on the intensity of C N valence vibrations in aromatic Schiff bases. Spectrochimica Acta Part A: Molecular and Biomolecular Spectroscopy, 51(14): 2517-2523.

Landau, L. D. and Lifshitz, E. M. 1976. Mechanics (3rd ed.). Pergamon Press, 167 page, India.

L'Annunziata, M. F. 2007. Radioactivity: introduction and history. Elsevier BV. pp. 55–58, Netherlands.

Laufer, G. 1996. Introduction to optics and lasers in engineering. Cambridge University Press, 476 page, USA.

Lavanya, R. 2017. Sulphonamides: a pharmaceutical review. International Journal of Pharmaceutical Science Invention, 6 (2): 1-3.

Leach, A. R. 2001. Molecular modelling: principles and applications. Pearson education, 727 page, USA.

Lehtola, S. 2019. A review on non- relativistic, fully numerical electronic structure calculations on atoms and diatomic molecules. International Journal of Quantum Chemistry, 119(19): 25968.

Leppilampi, M., 2006. "Functional and immunohistological studies on cancerassociated carbonic anhydrase IX". Ph.D Thesis, Faculty of Medicine, 60 page, Finland.

Levy, M. 1979. Universal variational functionals of electron densities, first-order density matrices, and natural spin-orbitals and solution of the v-representability. problem. Proceedings of the National Academy of Sciences, 76(12): 6062-6065.

Liew, S. C. 2006. Electromagnetic Waves. Centre for Remote Imaging, Sensing and Processing, 4: 24-28.

Maren, T. H. 1967. Carbonic anhydrase: chemistry, physiology, and inhibition. Physiological reviews, 47(4): 595-781.

McWeeny, R. and Sutcliffe, B. T. 1985. Fundamentals of self-consistent-field (SCF), Hartree-Fock (HF), multi-configuration (MC) SCF and configuration interaction (CI) schemes. Computer Physics Reports, 2(5): 219-278.

Meyers, F., Jawetz, H. E., and Goldfien, A. 1972. Review of Medical Pharmacology, 3rd ed.,Lange Medical Publications, 3: 523–527.

Mlynarek, V. 1986. Progr. NMR Spectrosc. 18: 277-305.

Moeker, J., Peat, T. S., Bornaghi, L. F., Vullo, D., Supuran, C. T. and Poulsen, S. A. 2014. Cyclic secondary sulfonamides: unusually good inhibitors of cancer-related carbonic anhydrase enzymes. Journal of medicinal chemistry, 57(8): 3522-3531.

Ng, L. M. and Simmons, R. 1999. Infrared spectroscopy. Analytical chemistry, 71(12): 343-350.

Novelline, R. 1997. Squire's Fundamentals of Radiology. Harvard University Press, 1074 page,UK.

Oh, S. W., Weiss, J. W., Kerneghan, P. A., Korobkov, I., Maly, K. E. and Bryce, D. L. 2012. Solid- state 11B and 13C NMR, IR, and X- ray crystallographic characterization of selected arylboronic acids and their catechol cyclic esters. Magnetic Resonance in Chemistry, 50(5): 388-401.

Özbek, N., Alyar, S., Memmi, B. K., Gündüzalp, A. B., Bahçeci, Z. and Alyar, H. 2017. Synthesis, characterization, computational studies, antimicrobial activities and carbonic anhydrase inhibitor effects of 2-hydroxy acetophenone-N-methyl p-toluenesulfonylhydrazone and its Co (II), Pd (II), Pt (II) complexes. Journal of Molecular Structure, 1127: 437-448.

Özensoy, Ö. 2002. Eritrositlerden karbonik anhidraz izoenzimlerinin saflaştırılması için yeni bir afinite jelinin sentezi ve uygulanması. Master's thesis, Balıkesir Üniversitesi, 64 page, Balıkesir.

Penning, T. D., Talley, J. J., Bertenshaw, S. R., Carter, J. S., Collins, P. W., Docter, S. and Isakson, P. C. 1997. Synthesis and biological evaluation of the 1, 5-diarylpyrazole class of cyclooxygenase-2 inhibitors: identification of 4-[5-(4-methylphenyl)-3-(trifluoromethyl)-1 H-pyrazol-1-yl] benzenesulfonamide (SC-58635, celecoxib). Journal of medicinal chemistry, 40(9): 1347-1365.

Pochareddy, S. A. 2019. DFT calculations for Cadmium Telluride (CdTe). Doctoral dissertation, Colorado State University, 73 page, USA.

Prasad, P. N. and Williams, D. J. 1991. Introduction to nonlinear optical effects in molecules and polymers (Vol. 1). John Wiley and Sons, 302 page, New York

Rogalski, A. 2019. Infrared and terahertz detectors (3rd ed.). Boca Raton, FL: CRC Press, 1066 page, New York.

Roothaan, C. C. J. 1951. New developments in molecular orbital theory. Reviews of modern physics, 23(2): 69.

Scaccia, S. and Goszczynska, B. 2004. Sequential determination of platinum, ruthenium, and molybdenum in carbon-supported Pt, PtRu, and PtMo catalysts by atomic absorption spectrometry. Talanta, 63(3): 791-796.

Schlegel, H. B. and Frisch, M. J. 1995. Transformation between Cartesian and pure spherical harmonic Gaussians. International Journal of Quantum Chemistry, 54(2): 83-87.

Schrader, B. 1995. Infrared and Raman Spectroscopy: Methods and Applications. VCH, Weinheim, 787 page, New York

Schrödinger, E. 1926. An undulatory theory of the mechanics of atoms and molecules. Physical review, 28(6): 1049.

Scozzafava, A., Mastrolorenzo, A. and Supuran, C. T. 2000. Arylsulfonyl-N, N-diethyl-dithiocarbamates: a novel class of antitumor agents. Bioorganic & medicinal chemistry letters, 10(16): 1887-1891.

Sidhu, P. S., Liang, A., Mehta, A. Y., Abdel Aziz, M. H., Zhou, Q. and Desai, U. R. 2011. Rational design of potent, small, synthetic allosteric inhibitors of thrombin. Journal of medicinal chemistry, 54(15): 5522-5531.

Silva, A. M., Sousa, R. M., Jimeno, M. L., Blanco, F., Alkorta, I. and Elguero, J. 2008. Experimental measurements and theoretical calculations of the chemical shifts and coupling constants of three azines (benzalazine, acetophenoneazine and cinnamaldazine). Magnetic Resonance in Chemistry, 46(9): 859-864.

Singh, H., Srivastava, V. K., Shukla, S. N., Srivastava, M. K. and Upadhyay, M. K. 1994. Synthesis, characterization and fungitoxicity of manganese (II), iron (II), cobalt (II), nickel (II), copper (II) and zinc (II) complexes of N-phenyl-5-phenyl-1, 3, 4oxadiazole-2-sulphonamide and 5-phenyll, 3, 4-oxadiazole-2-imino sulphonamide. NISCAIR-CSIR, 33: 350-353.

Skoog, D. A., Holler, J. F. and Crouch, S. R. 2007. Principles of Instrumental Analysis. Section Three-Molecular Spectroscopy: Chapter 13: An introduction to ultraviolet-visible molecular absorption spectrometry. Chapter 14: Applications of ultraviolet-visible molecular absorption spectrometry. Chapter 16: An introduction to infrared spectrometry. Chapter 17: Applications of infrared spectrometry. Thomson, 2: 335-398.

Slater, J. 1929. "The Theory of Complex Spectra". Physical Review. 34 (2): 1293–1322.

Slater, J. C. 1960. Quantum theory of atomic structure, Vol. 1, McGraw-Hill Book Company, 53 page, New York.

Sommerfeld, T. 2011. Lorentz trial function for the hydrogen atom: a simple, elegant exercise. Journal of Chemical Education, 88(11): 1521-1524.

Sparkman, O. D. 2000. Mass spectrometry desk reference 2. Journal of the American Society for Mass Spectrometry, 12(11): 1138-1144.

Sundaraganesan, N., Kavitha, E., Sebastian, S., Cornard, J.P. and Martel, M. 2009. Experimental FT-IR, FT-IR (gas phase), FT-Raman and NMR spectra., Hyperpolarizability studies and. DFT calculations of. 3,5-dimethylpyrazole, Spectrochim. Acta, Part A, 74: 788-797.

Supuran, C. T., Scozzafava, A., Casini, A., 2003 "Carbonic Anhydrase Inhibitors", Medicinal research reviews, 23: 146-189.

Tarun, A. S., Bryant, B., Zhai, W., Solomon, C. and Shusterman, D. 2003. Gene expression for carbonic anhydrase isoenzymes in human nasal mucosa. Chemical senses, 28(7): 621-629.

Teng, Q. 2012. Structural biology: practical NMR applications. Springer Science and Business Media, 434 page, USA.

Thøgersen, L., Olsen, J., Yeager, D., Jørgensen, P., Sałek, P. and Helgaker, T. 2004. The trust-region self-consistent field method: Towards a black-box optimization in Hartree–Fock and Kohn–Sham theories. The Journal of chemical physics, 121(1): 16-27.

Uzan, J. P., Leclercq, B. and Mizon, B. 2008. The natural laws of the universe: understanding fundamental constants Springer, pp. 43-44, New York.

Vainshtein, L. A. 1988. Electromagnetic waves. Moscow Izdatel Radio Sviaz, 440 page, Russian.

Villard, P. 1900. Sur la réflexion et la réfraction des rayons cathodiques et des rayons déviables du radium. Comptes rendus, 130: 1010–1012.

Wacker, M. and Holick, M. F. 2013. Sunlight and Vitamin D: A global perspective for health. Dermato-endocrinology, 5(1): 51-108.

Wojciechowski, P. M. and Michalska, D. 2007. Theoretical Raman and infrared spectra, and vibrational assignment for para-halogenoanilines: DFT study. Spectrochimica Acta Part A: Molecular and Biomolecular Spectroscopy, 68(3): 948-955.

Wolff, M. E. 1996. Burger's medicinal chemistry and drug discovery. American Journal of Therapeutics, 3(8): 608.

Yeşilkaynak, T., Binzet, G., Emen, F. M., Flörke, U., Külcü, N., Arslan, H. 2010. Theoretical and experimental studies on N-(6-methylpyridin-2-yl-carbamothioyl) biphenyl-4-carboxamide. European Journal of Chemistry, 1(1): 1-5.

Zeitler, J. A., Taday, P. F., Newnham, D. A., Pepper, M., Gordon, K. C. and Rades, T. 2007. Terahertz pulsed spectroscopy and imaging in the pharmaceutical setting- a review. Journal of Pharmacy and Pharmacology, 59(2): 209-223.

CURRICULUM VITAE

Personal Information

Name and Surname : Hasanain Abdulkareem Abbas AL-HADMAWI

Education

MSc	Çankırı Karatekin University Graduate School of Natural and Applied Sciences Department of Physics	2020-Present
Undergraduate	Babylon University College of Educatıon For Pure Sciences Department of Physics	2012-2016